NUMERICAL STUDY OF HEAT TRANSFER PERFORMANCE OF SUSPENSION OF NANOFLUIDS IN HEAT EXCHANGER TUBE

ROSMAWATI BINTI MAT JIHIN

SUBMITTED TO THE
FACULTY OF ENGINEERING
UNIVERSITY OF MALAYA, IN PARTIAL FULFILMENT
OF THE REQUIREMENT FOR THE DEGREE OF
MASTER OF MECHANICAL ENGINEERING

2013

UNIVERSITI MALAYA

ORIGINAL LITERARY WORK DECLARATION

Name of Candidate: **ROSMAWATI MAT JIHIN**

Registration/Matric No: **KGY 110025**

Name of Degree: **MASTER OF MECHANICAL ENGINEERING**

Title of Project Paper/Research Report/Dissertation/Thesis ("this Work"):

NUMERICAL STUDY OF HEAT TRANSFER PERFORMANCE OF SUSPENSION OF NANOFLUIDS IN HEAT EXCHANGER TUBE

Field of Study: **HEAT AND MASS TRANSFER**

I do solemnly and sincerely declare that:

(1) I am the sole author/writer of this Work;
(2) This Work is original;
(3) Any use of any work in which copyright exists was done by way of fair dealing and for permitted purposes and any excerpt or extract from, or reference to or reproduction of any copyright work has been disclosed expressly and sufficiently and the title of the Work and its authorship have been acknowledged in this Work;
(4) I do not have any actual knowledge nor do I ought reasonably to know that the making of this work constitutes an infringement of any copyright work;
(5) I hereby assign all and every rights in the copyright to this Work to the University of Malaya ("UM"), who henceforth shall be owner of the copyright in this Work and that any reproduction or use in any form or by any means whatsoever is prohibited without the written consent of UM having been first had and obtained;
(6) I am fully aware that if in the course of making this Work I have infringed any copyright whether intentionally or otherwise, I may be subject to legal action or any other action as may be determined by UM.

Candidate's Signature Date

Subscribed and solemnly declared before,

Witness's Signature Date

Name:

Designation:

ABSTRACT

This study was focus on the flow separation phenomena of annular passage which appears in a number of flow situations. It practically observed to cause recirculation flows that will affect the amount of heat transfer rate in several engineering application. The primary aim of this study is to identify the performance of three type of nanofluids : Al_2O_3 at 0.5%, 1% and 2% volume fractions and CuO and TiO_2 at 2% concentration over the base fluid water. The model considered is an annular passage with sudden expansion, having a constant step height, s=13.5mm for Al_2O_3 and TiO_2 and various step height , s=6mm, 13.5mm and 18.5mm for CuO uniformly heated with constant heat flux, q=49050 W/m^2. This geometries is evaluated and simulated using CFD software package ANSYS 14.0. The solver used standard k-ε turbulence model in calculating the solution for the flow field given by Reynolds number 17050, 302720, 39992 and 44545 for both uniform flow and fully developed turbulent flow. The investigation shows that the increase of Reynolds number will reduce the surface temperature at the reattachment zone. The lowest temperature will occur at this area and shows the location of reattachment point. The surface temperature will increase gradually with the pipe distance for all the nanofluids applied.

ABSTRAK

Kajian ini memberi tumpuan kepada fenomena pemisahan aliran laluan anulus yang muncul dalam beberapa situasi aliran. Ia sering diperhatikan kerana selalu menyebabkan aliran peredaran semula yang akan memberi kesan kepada jumlah kadar pemindahan haba dalam beberapa aplikasi kejuruteraan. Tujuan utama kajian ini adalah untuk mengenal pasti prestasi tiga jenis bendalir nano, iaitu: Al_2O_3 dengan kepekatan 0.5%, 1% and 2% serta CuO dan TiO_2 dengan kepekatan 2% berbanding cecair asas iaitu air. Model untuk analisis ini dianggap sebagai laluan anulus dengan perkembangan tiba-tiba, yang mempunyai ketinggian malar langkah, s = 13.5mm bagi Al_2O_3 dan TiO_2 serta variasi ketinggian langkah bagi CuO iaitu, s=6mm, 13.5mm dan 18.5mm yang dipanaskan secara seragam dengan fluks haba, q = 49050 W/m^2. Geometri ini dinilai dan disimulasi menggunakan kaedah pengkomputeran bendalir dinamik(CFD) menggunakan pakej perisian ANSYS 14.0. Penyelesaian menggunakan model k-ε gelora dalam pengiraan penyelesaian untuk medan aliran yang diberikan oleh nombor Reynolds 17050, 302720, 39992 dan 44545 bagi kedua-dua aliran seragam dan aliran gelora maju. Siasatan menunjukkan bahawa peningkatan nombor Reynolds akan mengurangkan suhu permukaan di zon penyambungan itu. Suhu terendah akan berlaku pada bahagian ini dan menunjukkan lokasi titik penyambungan itu. Suhu permukaan akan meningkat secara beransur-ansur dengan jarak paip untuk semua bendalir nano digunakan.

ACKNOWLEDGEMENTS

I would like to express my gratitude to my advisor, Dr. Kazi Salim Newaz for all of his guidance, encouragement, direction and patience with me through my time as a graduate student at University of Malaya since 2012. In addition, I would also like to thank the members of my coursework study for all of their guidance and input during the research process. In addition, I would also like to thank Mr. C.S. Oon from Department of Mechanical Engineering UM for his recommendations in the use of ANSYS FLUENT, as I had essentially no experience in this program prior to this research.

Finally, I would like to extend my utmost gratitude to my family and friends, who have supported and encouraged me during my time as a student at University Malaya. I would like to especially thank my husband Mr Ahmad Badrul Hisham bin Norazmir, for his full commitment and dedicated to take care over my son Darish Ziqran and my daughter Darin Zalyqha very well during my hard time in this journey and my parents for their unwavering support, as I would not be where I am today without them.

TABLE OF CONTENTS

LIST OF FIGURES

LIST OF TABLES

NOMENCLATURE

γ	Specific Gravity of Fluid
ε	Turbulent dissipation
μ	Dynamic Viscosity of Fluid
ρ	Density of Fluid
ν	Kinematic Viscosity of Fluid
σ_k	Computational constant for turbulent kinetic energy
σ_ε	Computational constant for turbulent dissipation
in	Inches
k	Turbulent kinetic energy
k	Thermal conductivity
T	Absolute Temperature of Fluid
u	Velocity in the x-direction
u_i	Velocity in the i-direction, where i is a Cartesian component
v	Velocity in the y-direction
q	Heat flux
L	Characteristic Length

CHAPTER 1:INTRODUCTION

A progressive attention has been given to the nanofluids for enhancing the coolant performance due to the formation of heat flux from electronic chips, automotive system or production industry. Vital consideration to increase the heat transfer rate has become the main objectives of previous studies as various findings from experimental and numerical study showed the capability of this type of fluids. The suspended of particle such as silica, alumina, copper dioxide, etc. into the based fluid like water required more understanding in order to determine the thermophysical properties of the fluids. Due to the observed improvement in the thermal conductivity, nanofluids are expected to provide enhanced convective heat transfer. This study was focus on the flow separation phenomena of annular passage which appears in a number of flow situations. It practically observed to cause recirculation flows that will affect the amount of heat transfer rate in several engineering application. The simulation of this study will then shows the distribution of temperature along the annular passage by applying nanofluids as a cooling medium inside the test tube. The application of heat exchanger tube expansion practically observed in fluid machineries of process plant or nuclear plant.

1.1 Nanofluids

Nanofluids have come into attention, since they display higher potential as heat transfer fluid than normally utilized base fluids and micron sized particle-fluids. This is due to clogging in pumping and flow apparatus which is caused by rapid settling of the micron sized particle. Nanofluids do not indicate this behavior. This makes nanofluids a better choice as heat transfer fluid (Roberts & Walker 2010).

Nanofluids (1-100nm-size particles), often called as suspension, are stable and prepared by dispersing a certain percentage of nanoparticles in base fluids (X. Wang &

Mujumdar 2006) (Roberts & Walker 2010) (Ghadimi et al. 2011). There are two different ways to prepare the nanofluids, namely single-step and two-step method. The single-step method involves direct evaporation and the technique is called Vacuum Evaporation onto a Running Oil Substrate (VEROS). Whereas in two-step method, nanoparticles are firstly produced and they are then dispersed in the host fluids like water, mineral oil or glycol (X. Wang & Mujumdar 2006) (Saidur et al. 2011).

One-step technique can reduce nanoparticle agglomeration, but is only compatible with low vapor pressure fluids. Two-step technique is more widely used since nanopowders are commercially available. However, this method functions well for oxide nano-scale particles, but does not work well with metal particles (X. Wang & Mujumdar 2006).

Among the main factors which causes heat transfer enhancement are solid particles and host fluids chemical composition, size, shape and concentration of nanoscale particles, thermal condition and surfactants. Some of these factors also affect the stability of the nanofluids. There are three strategies to attain good stability, namely addition of surfactants, pH control and ultrasonification (Ghadimi et al. 2011).

Number of carried out test should not be overlooked for stability measurement and the minimum number of repeating the test should be three times with various stability measurements such as zeta potential test and SEM (Scanning Electron Microscopy) test to assure that the results are reliable. However, it is essential to note that the stability does not guarantee the heat transfer enhancement (Ghadimi et al. 2011). The lack of stability of the nanofluids will lead to erosion and high flow resistance(Wang & Mujumdar, 2006). Current trend in producing smaller and lighter heat exchanger will be supported by the employment of nanofluids to the system.

1.2 Separated flow of annular passage

The flow separation practically importance in many engineering applications such as cooling electronic equipment, combustion chambers, cooling of nuclear reactors, high performance heat exchangers, energy systems equipment, and collector of power systems. The reattachment and separation occur due to the flow over of backward facing or forward facing step of the fluids in heating and cooling applications. In some circumstances, separation flow maybe encouraged, such as in burner flame stabilization use to enhanced mixing and heat transfer rate. However, numerous occurrences regarding this flow leads to energy losses and undesirable pressure drops which entailed high pumping power (A. Al-aswadi et al. 2010)

Substantial expansion of local heat transfer rate may occur at the reattachment region. The variation of step height effect the amount of heat transfer at the separation area proportionally but a little effect in redevelopment area. The local heat transfer coefficient increases up to the maximum value at the reattachment point and then decreases gradually in the redevelopment region.(Togun et al. 2011). The sudden change at the step edge caused the downstream flow to behave like a free shear layer, where the top side of the layer flow with higher speed compared to the below layer (Nait Bouda et al. 2008).

The study of backward facing step is of particular interest as it provided an exceptional flow for studying the behavior of separation and reattachment, as shown in Figure 1.1. The flow parameters deal with the study are the boundary layer thickness δ, developed at the height h of the backward facing step flow. The reattachment of flow will give an impact to the velocity and temperature distribution as it flow through the stream. The factors such as Reynolds number, heat flux, and fluid thermophysical properties will affects the performance of fluid heat transfer rate.

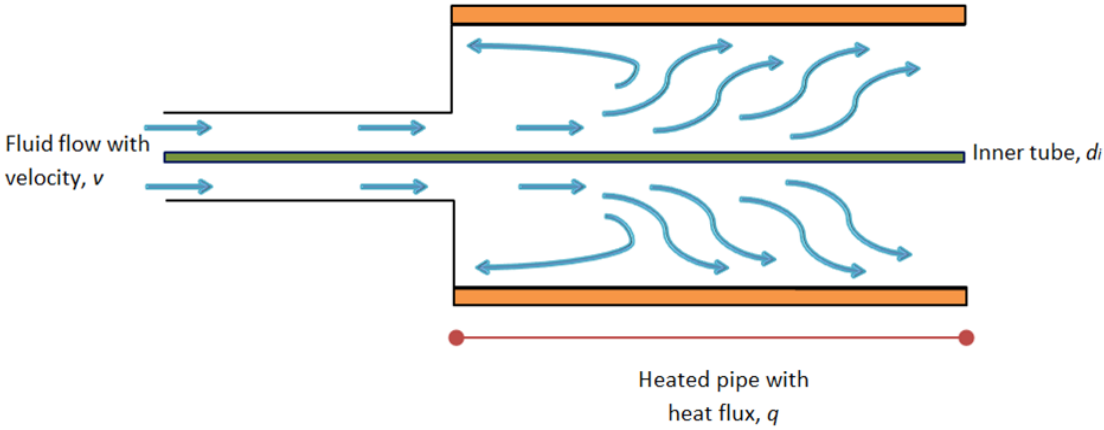

Figure 1.1:Fluid behaviour for backward facing step in separated flow

The measurements of temperature and fluid velocity at any location for experimental studies normally used the Laser Doppler speedometer and anemometer(H. a. Mohammed et al. 2011). For numerical investigation, the model configuration for the step and boundary condition were designed approximately using Design Modeller in Ansys Workbench or Gambit. The Boussinesq approximation applied to the flow that assumed to be in steady state mode. The equation to describe mass conservation, momentum and energy equation for the heat transfer problem occur to the system simplified as follows(Saldana et al. 2005a):

Continuity equation:

$$\frac{\partial(\rho u)}{\partial x}+\frac{\partial(\rho v)}{\partial y}+\frac{\partial(\rho w)}{\partial z}=0 \tag{1}$$

X-Momentum equation:

$$u\frac{\partial(\rho u)}{\partial x}+v\frac{\partial(\rho u)}{\partial y}+w\frac{\partial(\rho u)}{\partial z} = -\frac{\partial P}{\partial x}\left[\frac{\partial}{\partial x}\left(\mu\frac{\partial u}{\partial x}\right)+\frac{\partial}{\partial y}\left(\mu\frac{\partial u}{\partial y}\right)+\frac{\partial}{\partial z}\left(\mu\frac{\partial u}{\partial z}\right)\right] \tag{2}$$

Y-Momentum equation:

$$u\frac{\partial(\rho v)}{\partial x}+v\frac{\partial(\rho v)}{\partial y}+w\frac{\partial(\rho v)}{\partial z}=-\frac{\partial P}{\partial y}+\rho_o\beta(T-T_o)g_y = \left[\frac{\partial}{\partial x}\left(\mu\frac{\partial v}{\partial x}\right)+\frac{\partial}{\partial y}\left(\mu\frac{\partial v}{\partial y}\right)+\frac{\partial}{\partial z}\left(\mu\frac{\partial v}{\partial z}\right)\right] \tag{3}$$

Z-Momentum equation:

$$u\frac{\partial(\rho w)}{\partial x}+v\frac{\partial(\rho w)}{\partial y}+w\frac{\partial(\rho w)}{\partial z}$$
$$=-\frac{\partial P}{\partial z}\left[\frac{\partial}{\partial x}\left(\mu\frac{\partial w}{\partial x}\right)+\frac{\partial}{\partial y}\left(\mu\frac{\partial w}{\partial y}\right)+\frac{\partial}{\partial z}\left(\mu\frac{\partial w}{\partial z}\right)\right] \quad (4)$$

Energy equation:

$$u\frac{\partial(\rho C_p T)}{\partial x}+v\frac{\partial(\rho C_p T)}{\partial y}+w\frac{\partial(\rho C_p T)}{\partial z}$$
$$=\left[\frac{\partial}{\partial x}\left(k\frac{\partial T}{\partial x}\right)+\frac{\partial}{\partial y}\left(k\frac{\partial T}{\partial y}\right)+\frac{\partial}{\partial z}\left(k\frac{\partial T}{\partial z}\right)\right] \quad (5)$$

The study of heat transfer enhancement in backward facing step mostly considered based on the development of basic features like reattachment, recirculation, separations of the shear layer(Abu-Nada 2008). To discretize the momentum and energy equation, the implementation of finite volume were required. The power law denoted solution for the convection diffusion equation appeared at the control volume interface. Link to the pressure and velocity fields of a system executed by using SIMPLE algorithm(Saldana et al. 2005b).

The effect of step inclined angle much more studied by the researcher to examine the correlation with the reattachment length. The unsteadiness and pressure fluctuation due to the separation appeared to be different between all the angles. With the increase of step inclined angle, the reattachment point also increase until 45^{o} and approximately constant afterwards(Singh et al. 2011). The reattachment line encountered high influence from the Reynolds number when the value of expansion ratio(ER) increased, as shown in Figure 1.2

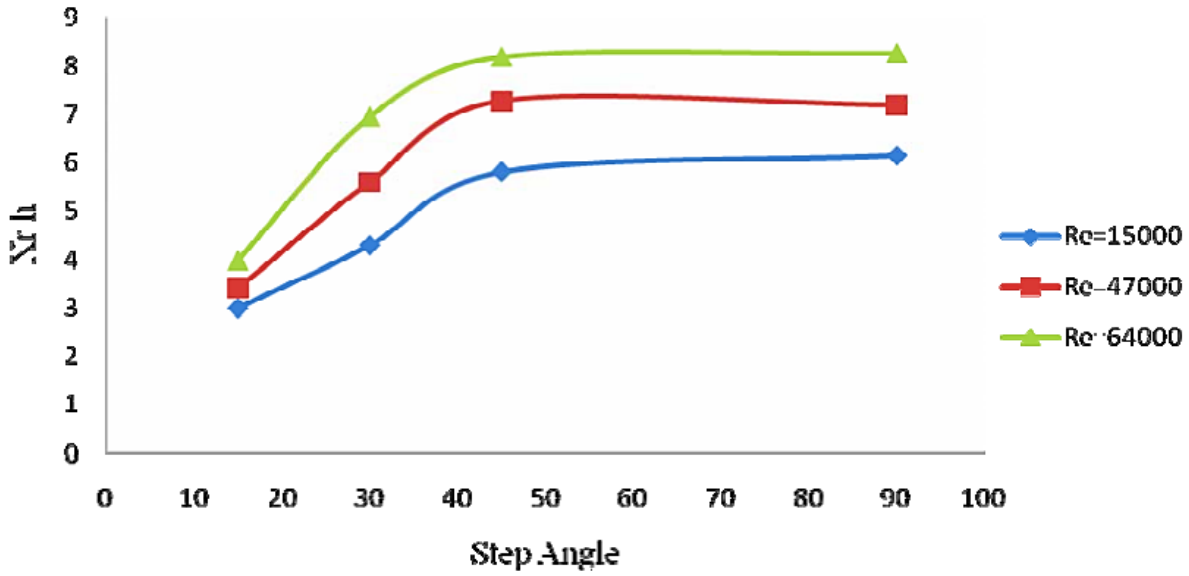

Figure 1.2: Relationship of reattachment length with the step angle (Singh et al., 2011)

1.3 Turbulent Convective Heat Transfer

The fluid passing through the cylindrical pipe used to flow either in laminar or turbulent form. The separated flow caused by the step will generate boundary layer at the pipe wall. Upstream disturbances has not been established as a feature affected the friction factor whether the flow in the phase of laminar, turbulent or transitional(Bhandari 2012). Turbulent flow dictated by the eddies which expectable and less structured. The flow almost impossible to solve analytically due to the rotation and mixing cause by the eddies to the flow. The size of the eddies ranging from the whole width of boundary layer until the microscopic structures(Stolpa 2004).

The characteristic of turbulence has always been the main focus by many researchers in order to get better understanding of turbulent flow. Due to the uncertainty of the behavior, researchers must rely on the idealized of turbulent and laminar model for the investigation. In the system of equations for the turbulent flow, the unknowns appeared to be more than the equations. In order to solve this

problems, assumptions was created to reduce the number of unknowns but it was not all faultless. A lot of studies proposed to improve this model while the computer software relies on the accuracy of the models. The high value of Reynolds number typically represents turbulent flow. When roughness added to the system surface, the transition flow to turbulence will be appeared through methods like stumbling in easily(W. Wang et al. 2012).

In simulation of turbulent flow, the k-epsilon model has been used comprehensively. But, some researchers have shown that the model failed to predict the heat transfer characteristics especially in separated region of flow (Lan et al. 2009). The conforming boundary conditions and governing equation for the turbulence forced convection flow shown in the equations below:

$$\frac{\partial \rho U_i}{\partial x_i} = 0$$

$$\frac{\partial}{\partial x_j}\left(\rho U_i U_j\right) = -\frac{\partial p}{\partial x_i} + \frac{\partial}{\partial x_j}\left[(\mu + \mu_t)\left(\frac{\partial U_i}{\partial x_j} + \frac{\partial U_j}{\partial x_i}\right)\right] \tag{6}$$

$$\frac{\partial}{\partial x_j}\left(\rho U_j \bar{T}\right) = \frac{\partial}{\partial x_j}\left(\left(\frac{\mu}{Pr} + \frac{\mu_t}{Pr}\right)\frac{\partial \bar{T}}{\partial x_j}\right) \tag{7}$$

$$\frac{\partial}{\partial x_j}\left(\rho U_j k\right) = \frac{\partial}{\partial x_j}\left[(\mu + \mu_t)\frac{\partial k}{\partial x_j}\right] + G_k - \rho\epsilon \tag{8}$$

$$\frac{\partial}{\partial x_j}\left(\rho U_j \epsilon\right) = \frac{\partial}{\partial x_j}\left[\left(\mu + \frac{\mu_t}{1.3}\right)\frac{\partial \epsilon}{\partial x_j}\right] + \frac{C_{\epsilon 1} G_k + 1.9\rho\epsilon}{T} \tag{9}$$

$$\frac{\partial}{\partial x_j}\left(\rho U_j \zeta\right) = \frac{\partial}{\partial x_j}\left[\left(\mu + \frac{\mu_t}{1.2}\right)\frac{\partial \zeta}{\partial x_j}\right] + \rho f - \frac{\zeta G_k}{k} \tag{10}$$

$$L_t^2 \nabla^2 f - f - \frac{1}{T}\left(0.4 + \frac{0.65 G_k}{\rho\epsilon}\right)\left(\zeta - \frac{2}{3}\right) = 0 \tag{11}$$

Where :

$$\mu_t = 0.22\zeta kT$$

$$C_{\epsilon 1} = 1.4\left(1.0 + \frac{0.012}{\zeta}\right)$$

$$T = max\left[min\left(\frac{k}{\epsilon}, \frac{0.6}{0.22\sqrt{3\zeta\bar{S}}}, 85\frac{v^3}{\epsilon}\right)^{0.25}\right]$$

$$L_t = 0.36\, max\left[min\frac{k^{1.5}}{\epsilon}, \frac{k^{0.5}}{0.22\sqrt{3\zeta\bar{S}}}, 85\left(\frac{v^3}{\epsilon}\right)^{0.25}\right]$$

$$\bar{S} = \sqrt{2_{ij}S_{ij}}$$

$$S_{ij} = \frac{\partial U_i}{\partial x_j} + \frac{\partial U_j}{\partial x_i}$$

$$G_k = (\mu_t)\left(\frac{\partial U_i}{\partial x_j} + \frac{\partial U_j}{\partial x_i}\right)\frac{\partial U_i}{\partial x_j}$$

All the variables will reach zero when approaching the wall, except ∈ and *f*.

The separation performs a greater effect on turbulent flow which is cause by the inertial effects. This condition frequently happens in any engineering application especially in the real case situation. The chances of separation occurrence are higher in turbulent flow compared to laminar flow. Those understanding are required in order to investigate the characteristics of flow regime that has a rapid variation and influenced by low momentum diffusion and high momentum convection(Prasad V.Tota 2009). The schematic flow pattern in Figure 1.3 shows that the separation point located behind the corner eddy,x_c with the mean reattachment point at x_r. The separation and reattachment at the roof wall assign with x_{t1} and x_{t2}, while at bottom wall with x_{b1} and x_{b2}. The wall shear rate calculations used to examine the extreme values and their localizations.

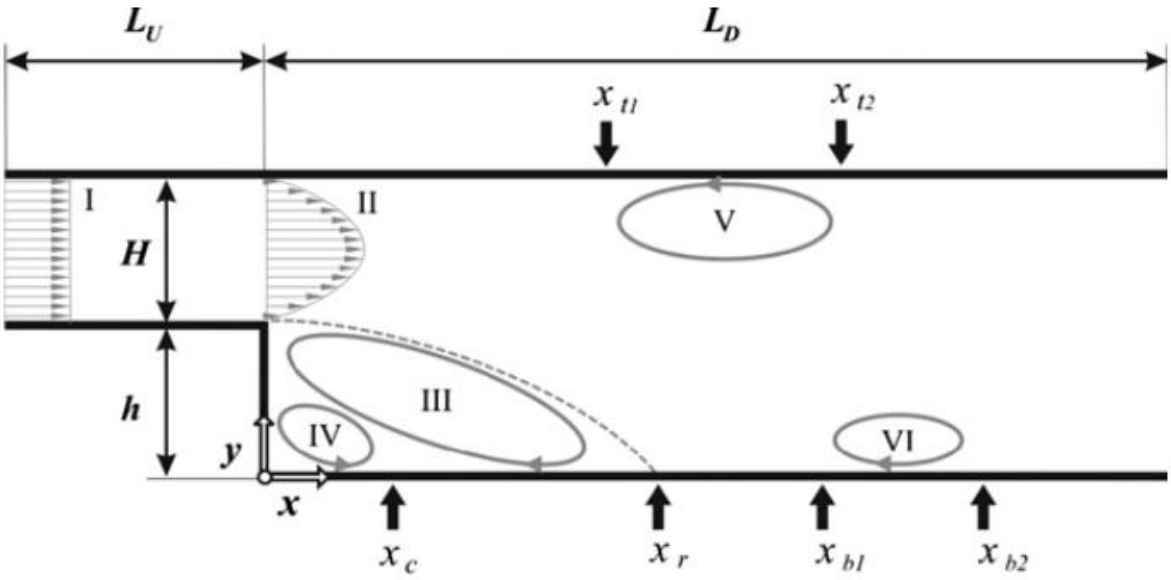

Figure 1.3:Model of a backward-facing step flow in 2D consists of : inlet flat velocity profile (I), parabolic velocity profile (II), mean recirculation region (III), corner eddy (IV), roof eddy (V), and secondary flow- recirculation at the bottom wall (VI)(Tihon et al. 2012)

1.4 Numerical Study

The study of algorithm and approximation from mathematical formulation extensively used by many researchers as an option in exploring the characteristics of fluid flow and heat transfer, other than experimental analysis. This type of investigation required no exact answer but concerned in approximate result that confined under an acceptable errors. The findings from numerical investigation will be compared with experimental value in order to verify the results. The study required an appropriate setting of boundary condition and model configuration before executing the simulation. The overall goal basically to design and analyze techniques to get approximate but accurate solutions to the complicated analysis. The outcomes from this finding will help to reduce cost and time that arise from the experimental study.

The flexibility of this method has become the main reason for it implementations. Since, engineering solution required various parametric variables, this methods seems to meet the specification. The procedures applied including: 1. Model configuration design 2. Material properties 3. Meshing 4. Computer simulation.

1.4.1 Model configuration design

The main techniques of numerical investigation for pre-processing phase is to model the system by using software like GAMBIT, ANSYS DesignModeler, Pro-E, AutoCAD or CATIA. This part is the most important part for the user to describe the exact model that will fulfill the requirement of the system. The cylindrical coordinates were used to solve an energy equations and simulation of the heated pipe. The flow is considered to be in steady state condition with the assumptions of no changes of flow in θ direction, thus allow the reduced of three-dimensional model to two-dimensional model(Gavtash et al. 2012).

1.4.2 Material properties

Next step is to identify the thermophysical properties of the material used. This value need to be inserted into the setup phase before in can be simulated. These properties will include thermal conductivity and diffusivity, heat capacity, thermal expansion and thermal radiative properties, as well as viscosity and mass and thermal diffusion coefficients, speed of sound, surface and interfacial tension in fluids. All this parameters affecting the heat transfer with the varies of temperature, pressure and composition without altering the material's chemical identity(Lancial et al. 2013)

The thermophysical properties of the nanofluids with variable of volume fractions(φ) of nanoparticles with the base fluid are determined using the following equations:

Density of nanofluid(Taylor n.d.):

$$\rho_{nf} = \varphi\rho_s + (1-\varphi)\rho \tag{12}$$

Effective thermal conductivity (Anderson 2001):

$$k_{nf} = \frac{k_p + (n-1)k_f - (n-1)\varphi\left(k_f - k_p\right)}{k_p + (n-1)k_f + \varphi(k_f - k_p} k_f \tag{13}$$

Specific heat of nanofluid(Xuan & Roetzel 2000):

$$\left(\rho C_p\right)_{nf} = (1-\varphi)\left(\rho C_p\right)_f + \varphi\left(\rho C_p\right)_p \tag{14}$$

Viscosity of nanofluid(Aminfar et al. 2010):

$$\mu_{nf} = \mu(1 + 2.5\varphi) \tag{15}$$

Where subscript *f,p,nf* correspond to fluid, particle and nanofluids. Nanoparticle shape factor(*n*) assumed to be 3 for spherical particles.

1.4.3 Meshing

A combine form of cells series, elements and nodes in computational fluid dynamics known as mesh. The meshing stages is the most crucial part as the accuracy of numerical calculations base on this phase. The shape of the cells and the node locations play a major role in calculating an accurate solution for fundamental equations of fluid dynamics and the simulation.

Two types of meshing currently used are:

1. Structured meshing,
2. Unstructured meshing

Structured meshing uses hexagonal shaped elements (12 edges and 8 nodes) while unstructured meshing uses tetrahedron shaped elements (6 edges and 4 nodes), as shown in Figure 1.4. Each method has advantages and disadvantages and it is imperative that the CFD user understands which meshing type is applicable for the given problem.

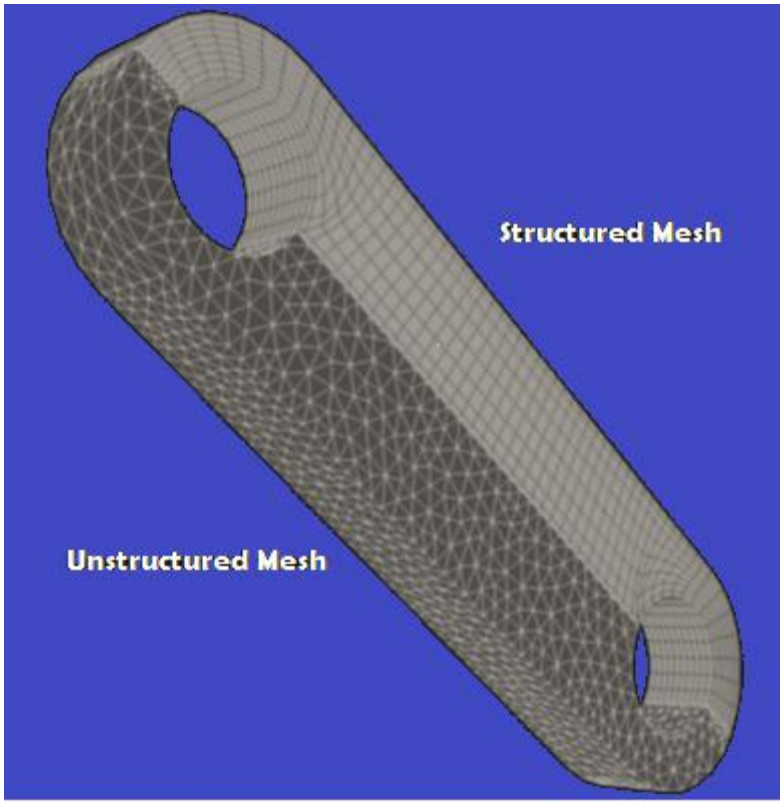

Figure 1.4: An example of structured and unstructured mesh

Mesh generation, in most cases is the timeliest task in the CFD simulation and can be quit challenging to generate a mesh that accurately defines the problem. Two available programs for this study are ANSYS CFX Mesh Generation which generates an unstructured mesh and ANSYS-ICEM CFD which can generate both a structured and unstructured mesh.

1.4.4 Computer Simulation

Computer simulation is a way of modeling complex fluid flow by breaking down geometry into cells that comprise a mesh. At each cell an algorithm is applied to compute the fluid flow for the individual cell. Depending on the nature of the flow either the Euler or Navier-Stokes equations can be used for the computation(Jonathan 2009). The investigation of fluid flow can be done by using an established computer, such as FLUENT to simulate the flow model.

In order to explain Fluent, once must understand the used of DesignModeler. DesignModeler is an application that is distributed along with FLUENT, as shown in Figure 1.5. As of this writing, it is owned and distributed by ANSYS, Inc.DesignModeler is used as a tool to generate or import geometry so that it can be used as a basis for simulations run in FLUENT. It can either build a model or import existing geometries from various various other CAD applications. With a geometry in place it generates a mesh for the surface and volume of the geometry allowing it to be used for computational fluid dynamics.

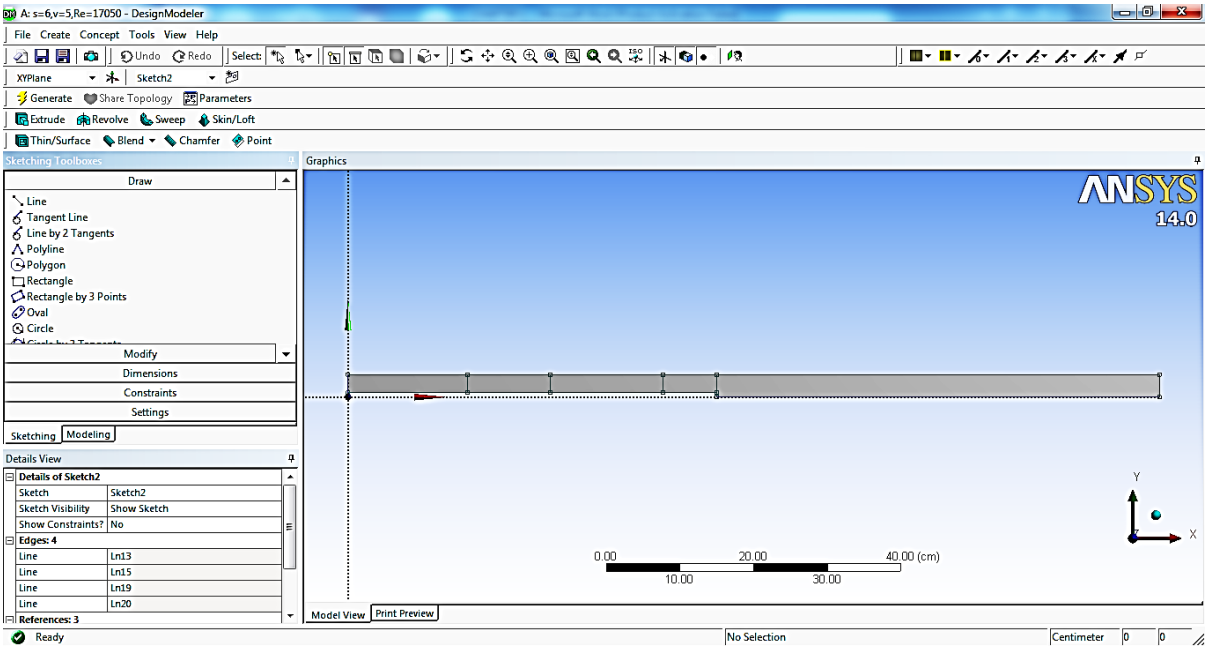

Figure 1.5: DesignModeler Interface

FLUENT is a “Flow Modeling Software” owned by and distributed by ANSYS, Inc. It is used to model fluid flow within a defined geometry using the rinciples of computational fluid dynamics. It is utilizes a multi window pane system for displaying various configuration menus and grids instead of a single window with several embedded sub-windows restricted within the space of the parent window, shown in Figure 1.6. FLUENT is able to read geometries generated in DesignModeler and model fluid flow within them. It can model various basic flow using computational fluid dynamics, including periodic flow, swirling and rotating flow, compressible flow and inviscid flow.

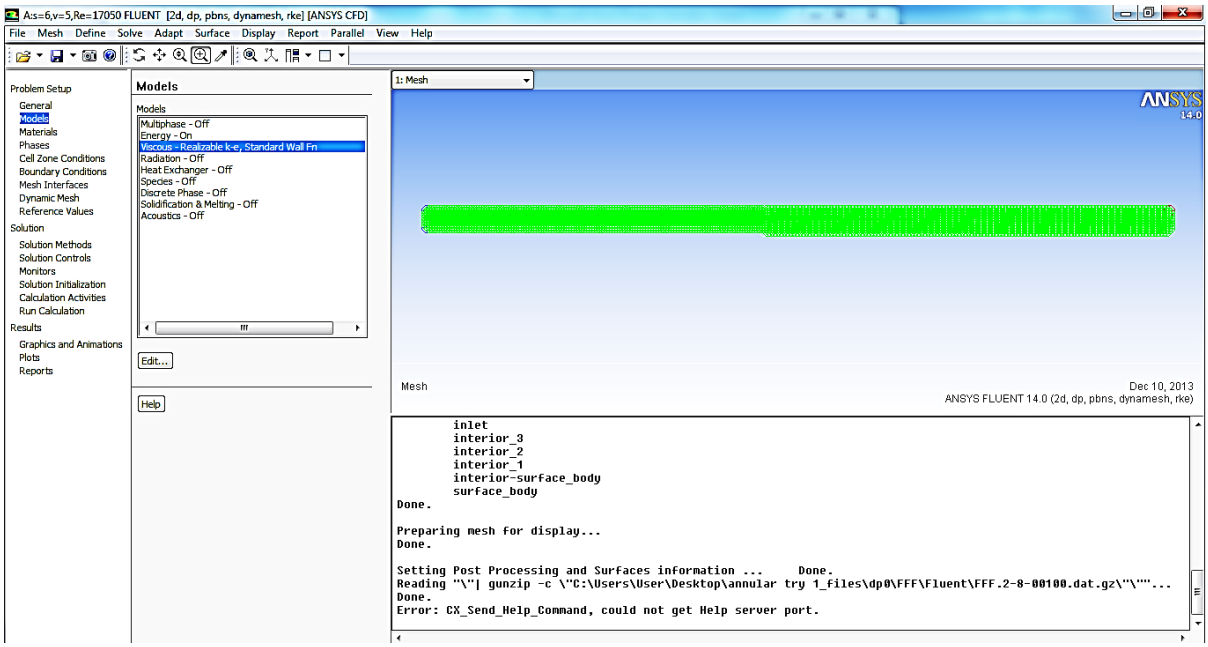

Figure 1.6: FLUENT Interface

Further explaination on the type of flow model described below(*ANSYS 14.0 Help*):

- Periodic Flow- Periodic flow occurs when the physical geometry of interest and the expected pattern of the flow/thermal solution have a periodically repeating nature. Two types of periodic flow can be modeled in ANSYS FLUENT. In the first type, no pressure drop occurs across the periodic planes. In the second type,

a pressure drop occurs across translationally periodic boundaries, resulting in "fully-developed" or "streamwise-periodic" flow

- Swirling and Rotating Flow - Many important engineering flows involve swirl or rotation and ANSYS FLUENT is well-equipped to model such flows. Swirling flows are common in combustion, with swirl introduced in burners and combustors in order to increase residence time and stabilize the flow pattern. Rotating flows are also encountered in turbomachinery, mixing tanks, and a variety of other applications.
- Compressible Flow - Compressibility effects are encountered in gas flows at high velocity and/or in which there are large pressure variations. When the flow velocity approaches or exceeds the speed of sound of the gas or when the pressure change in the system ($\Delta p/p$) is large, the variation of the gas density with pressure has a significant impact on the flow velocity, pressure, and temperature. Compressible flows create a unique set of flow physics for which you must be aware of the special input requirements.
- Inviscid Flow - Inviscid flow analysis neglect the effect of viscosity on the flow and are appropriate for high-Reynolds-number applications where inertial forces tend to dominate viscous forces. One example for which an inviscid flow calculation is appropriate is an aerodynamic analysis of some high-speed projectile. In a case like this, the pressure forces on the body will dominate the viscous forces. Hence, an inviscid analysis will give you a quick estimate of the primary forces acting on the body. After the body shape has been modified to maximize the lift forces and minimize the drag forces, you can perform a viscous analysis to include the effects of the fluid viscosity and turbulent viscosity on the lift and drag forces.

1.5 Objectives

The objectives of this study are:

1. To investigate the effect of flow separation in the heat exchanger tube.
2. To evaluate the thermophysical properties of the nanofluids (Al_2O_3,CuO and TiO_2).
3. To study the heat transfer performance of nanofluids (Al_2O_3,CuO and TiO_2) in backward facing step.

1.6 Scope of Study

This study attempts to investigate thermal performance of concentric annular heat exchanger tube using nanofluids based coolants. The study covered thermal conductivity and convective heat transfer coefficient based performance of concentric annular passage with concentration on the backward facing step at the test tube, which heated uniformly from the beginning of the expansion at constant heat flux. Various step size were used at the entrance of the test area to investigate the heat transfer performance for the selected nanofluid with fully developed turbulent flow. Nanoparticle used were alumina(Al_2O_3), copper oxide (CuO) and titanium dioxide(TiO_2) suspended in the water. The concentration of Al_2O_3 was varies in terms of it volume fraction to observe the effect of the deviation. The numerical observation carry out with the variation of nanofluids, Reynolds number and step height by using ANSYS Fluent for the heat transfer analysis .

CHAPTER 2: LITERATURE REVIEW

2.1 Turbulent Flow

Turbulence is the three-dimensional unsteady random motion observed in fluids at moderate to high Reynolds numbers. As technical flows are typically based on fluids of low viscosity, almost all technical flows are turbulent. Many quantities of technical interest depend on turbulence, such as:

- Mixing of momentum, energy and species
- Heat transfer
- Pressure losses and efficiency
- Forces on aerodynamic bodies

(Rostamani et al. 2010) studied the turbulent flow of nanofluids with different volume concentrations of nanoparticles flowing through a two-dimensional duct under constant heat flux condition. The nanofluids considered are mixtures of copper oxide (CuO), alumina (Al_2O_3) and oxide titanium (TiO_2) nanoparticles and water as the base fluid. All the thermophysical properties of nanofluids are temperature-dependent. The predicted Nusselt numbers exhibit good agreement with Gnielinski's correlation. The results show that by increasing the volume concentration, the wall shear stress and heat transfer rates increase. For a constant volume concentration and Reynolds number, the effect of CuO nanoparticles to enhance the Nusselt number is better than Al_2O_3 and TiO_2 nanoparticles.

(Roy et al. 2012) presents a numerical investigation of heat transfer and hydrodynamic behavior of various types of water-based nanofluids inside a typical radial flow cooling device. Turbulent radial nanofluid flow between two parallel disks with axial injection was considered in his study. Results show that although heat

transfer enhancement was found for all types of nanofluids considered, energy-based performance comparisons indicate that they do not necessarily represent the most efficient coolants for this type of application and flow conditions.

(Prasad V.Tota 2009) studied the turbulent flow over a backward-facing step to validate turbulence models in CFD. In their work, steady-state turbulent flow over a backward-facing step was simulated using FLOW-3D1 with the Renormalization-group (RNG) k-ε model to account for turbulent viscosity. The test case was run for two different Reynolds numbers: Re=5100 and Re=44,000. They found that, streamwise velocity profiles at different locations in the flow direction were in good agreement both qualitatively and quantitatively with the experimental results. The steady-state velocity was used to compute the reattachment length behind the step for different values of Reynolds number and have been compared with experimental data.

(Sajadi & Kazemi 2011) experimentally analyzed the turbulent heat transfer behavior of titanium dioxide/water nanofluid in a circular pipe with the volume fraction of nanoparticles in the base fluid was less than 0.25%. The results indicated that addition of small amounts of nanoparticles to the base fluid augmented heat transfer remarkably. There was no much effect on heat transfer enhancement with increasing the volume fraction of nanoparticles. The measurements also showed that the pressure drop of nanofluid was slightly higher than that of the base fluid and increased with increasing the volume concentration. A new correlation of the Nusselt number have been presented using the results of the experiments with titanium dioxide nanoparticles dispersed in water.

(Sundar & Sharma 2010) studied experimentally the turbulent convective heat transfer and friction factor behavior of Al_2O_3 nanofluid in a circular tube with different aspect ratios of longitudinal strip inserts. Results from their study, indicate that heat

transfer coefficients increase with nanofluid volume concentration and decrease with the aspect ratio, as shown in Figure 2.1 below.

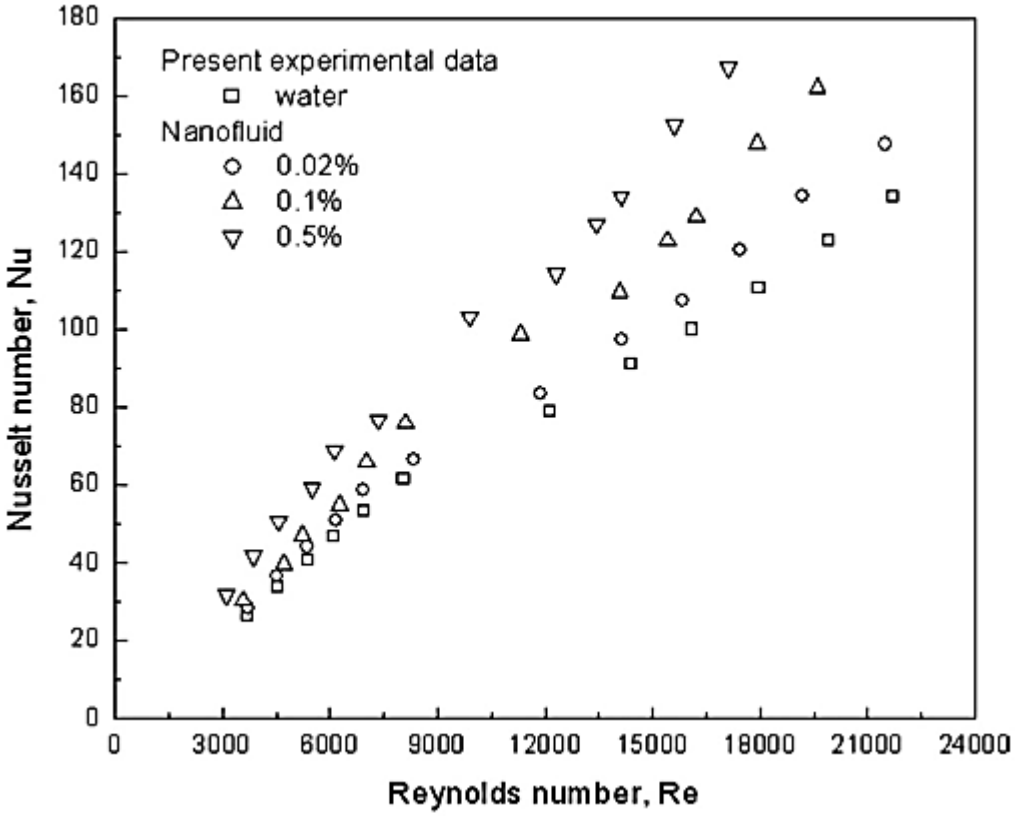

Figure 2.1: Effect of nanofluids concentration with Reynolds and Nusselt number(Sundar & Sharma, 2010)

(Yang et al. 2013) were performed an experimental studies to investigate the characteristics of convective heat transfer and flow resistance in turbulent pipe flows of viscoelastic fluid, water-based and viscoelastic-fluid-based nanofluids (VFBN) containing copper (Cu) nanoparticles. Experimental results of heat transfer and flow resistance indicated that the VFBN flows showed better heat transfer properties than viscoelastic base fluid flows and lower flow resistance s than water-based nanofluid flows. The convective heat transfer coefficients were increased with increase of temperature for all the tested flows, whereas temperature had no essential influence on pressure drop in the flows of Cu– water based nanofluid and VFBN.

2.2 Flow Expansion Phenomena

(Abu-Nada 2008) presenting a numerical investigation of heat transfer over a backward facing step (BFS), using nanofluids. The finite volume technique is used to solve the momentum and energy equations. He aws found in his study for the case of Cu nanoparticles, there was an enhancement in Nusselt number at the top and bottom walls except in the primary and secondary recirculation zones where insignificant enhancement is registered. It was found that outside the recirculation zones, nanoparticles having high thermal conductivity (such as Ag or Cu) have more enhancements on the Nusselt number. However, within recirculation zones, nanoparticles having low thermal conductivity (such as TiO_2) have better enhancement on heat transfer. An increase in average Nusselt number with the volume fraction of nanoparticles for the whole range of Reynolds number is registered.

(A. Al-aswadi et al. 2010) were numerically investigated a laminar forced convection flow of nanofluids over a 2D horizontal backward facing step placed in a duct using a finite volume method. A 5% volume fraction of nanoparticles is dispersed in a base fluid besides using various types of nanoparticles such as Au, Ag, Al_2O_3, Cu, CuO, diamond, SiO_2, and TiO_2. He was found that reattachment point moving downstream far from the step as Reynolds number increases. Nanofluid of SiO_2 nanoparticles is observed to have the highest velocity among other nanofluids types, while nanofluid of Au nanoparticles has the lowest velocity. The static pressure and wall shear stress increase with Reynolds number and vice versa for skin friction coefficient.

(Armalyt et al. 1983) reported the velocity distribution and reattachment length of a single backward-facing step mounted in a two-dimensional channel. The experimental results show that the various flow regimes are characterized by typical

variations of the separation length with Reynolds number. The high aspect ratio of the test section (1 : 36) ensured that the oncoming flow was fully developed and two-dimensional, the experiments showed that the flow downstream of the step only remained two-dimensional at low and high Reynolds numbers. The two-dimensional steady differential equations for conservation of mass and momentum were solved in his study. Results are reported for those Reynolds numbers for which the flow maintained its two-dimensionality in the experiments. Under the circumstances, good agreement have been achieved in his study between experimental and numerical investigation.

(Biswas et al. 2004) were concerned with the behavior of flows over a backward-facing step geometry for various expansion ratios H/h 1.9423, 2.5 and 3.0. Information on characteristic flow patterns is provided for a wide Reynolds number range, 10 $4 \leq ReD \leq 800$. The irreversible pressure losses are determined for various Reynolds numbers as a function of the expansion ratio. The two-dimensional simulations are known to underpredict the primary reattachment length for Reynolds numbers beyond which the actual flow is observed to be three-dimensional. This three-dimensional analysis with the same geometry and flow conditions reveals the formation of wall jets at the side wall within the separating shear layer. The wall jets formed by the spanwise component of the velocity move towards the symmetry plane of the channel. A self-similar wall-jet profile emerges at different spanwise locations starting with the vicinity of the side wall. The results complement information on backward-facing step flows that is available in the literature.

(Furuichi et al. 2004) carried out simultaneously a measurements of spatio–temporal velocity fields at the separated shear layer and reattachment region of a two-dimensional backward-facing step flow using a multi-point LDV. Figure 2.2 below

shows the results of the correlation of the velocity fluctuation, the moving path of the vortex shedding from the separated shear layer to the reattachment region exhibits two patterns which it moves to near the wall region or the middle of the step height at the reattachment region. Moreover, the turbulence concerned with reattachment phenomenon transports from the reattachment region to a separated shear layer by recirculation flow.

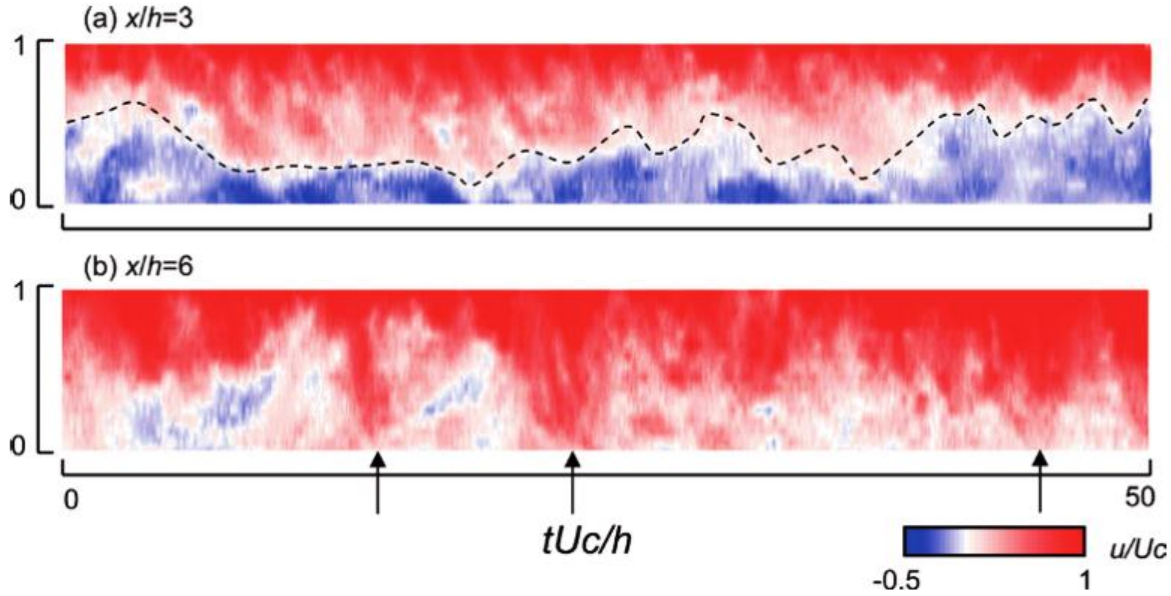

Figure 2.2:Diagram of spatio– temporal velocity field at x/h=3 and 6. The dot- ted line in (a) is the zero- velocity one(Furuichi et al., 2004)

(Oon et al. 2013) considered the separation and the reattachment of water flow through a sudden expansion in an annular passage in his study. In the study, the flowing fluid was considered heated uniformly from the beginning of the expansion, and the constant heat flux approach was also considered for the heat transfer investigation. The increase of flow reduces the surface temperature along the pipe to a minimum point, then gradually increases up to the maximum and hold for the rest of the pipe. The minimum surface temperature is obtained at flow reattachment point. He has observed that the position of the minimum temperature point is dependent on the flow velocity

over sudden expansion and the local Nusselt number (Nu) increases with the increase of Reynolds number, generally.

2.3 Thermal Resistance Study

(Teng et al. 2010) presents the enhancement of thermal efficiency of heat pipe charged with nanofluid in his study. The Al_2O_3/water nanofluid produced by direct synthesis method is used as the working fluid of experimental heat pipes with three different concentrations (0.5, 1.0 and 3.0 wt.%). The heat pipe is a straight copper tube with inner diameter and length of 8 and 600mm, respectively. The study discusses about the effects of charge amount of working fluid, tilt angle of heat pipe and weight fraction of nanoparticles on the thermal efficiency of heat pipe. According to the experimental results, the optimum condition of heat pipe is when nanoparticles being at 1.0 wt.%. Under this condition, the thermal efficiency is 16.8%, which is higher than that of heat pipe charged with distilled water. The charge amount can be decreased from 60% to 20%.

(Sonawane et al. 2011) are investigated Aviation Turbine Fuel (ATF)-Al_2O_3 nanofluids for better heat transfer performance in a potential application of regeneratively cooled semi-cryogenic rocket engine thrust chambers. The volume concentration of Al_2O_3 nanoparticles is varied between 0 and 1%. At 1% particle volume concentration, the enhancement in the thermal conductivity is 40%, whereas the viscosity increases by 38%. The measured specific heats of the nanofluids do not exhibit appreciable difference within the range of the particle volume concentrations investigated. The heat transfer coefficient increases by 30% at 1% particle volume concentration and correspondingly leads to an enhancement of 10% in the Nusselt number. For the same value of pressure drop, the heat transfer performances of nanofluids are compared with those of ATF. The experimental results showed that the

maximum enhancement in the heat transfer coefficient observed for the same pressure drop is 28% and even the least enhancement obtained is 2%.

(Rashmi et al. 2013) studied the used of carbon nanotube (CNT) nanofluids of 0.01 wt%, stabilised by 1.0 wt% gum arabic as a cooling liquid in a concentric tube laminar flow heat exchanger. The flow rate of cold fluid varied from 10 to 50 g/s. Both experimental and numerical simulations were carried out to determine the heat transfer enhancement using CNT nanofluids. The results showed thermal conductivity enhancement from 4% to 125% and nearly 70% enhancement in heat transfer with increase in flow rate. Numerical results exhibited good agreement with the experimental results with a deviation of 3:0%. CNT nanofluids at 0.01 wt% CNTs showed Newtonian behaviour with no significant increase in the density.

(Keshavarz Moraveji & Razvarz 2012) studied the effect of using aluminum oxide nanofluid (pure water mixed with Al_2O_3 nanoparticle with 35 nm diameter) on the thermal efficiency enhancement of a heat pipe on the different operating state. The heat pipe was made of a straight copper tube with an outer length of 8 and 190 mm and a 1 mm wick-thickness sintered circular heat pipe. In the heat pipe tube, there is a 90° curve between the evaporator and condenser sections. The tested concentration levels of nanofluid are 0%, 1% and 3%wt. Results show that by charging the nanofluid to the heat pipe, thermal performance is enhanced by reducing the thermal resistance and wall temperature difference.

(Gavtash et al. 2012) have modeled and simulate the effects of nanofluids on cylindrical heat pipes thermal performance using the ANSYS-FLUENT CFD commercial software in his research. The heat pipe outer wall temperature distribution, thermal resistance, liquid pressure and axial velocity in presence of suspended nanoscaled solid particle (i.e. Cu, Al_2O_3 and TiO_2) within the fluid (water) were

investigated. He has concluded that the thermal performance of the heat pipe is improved when using nanofluid as the system working fluid. Additionally, it was observed that the thermal resistance of the heat pipe drops as the particle concentration level increases and particle radius decreases, shown in Figure 2.3.

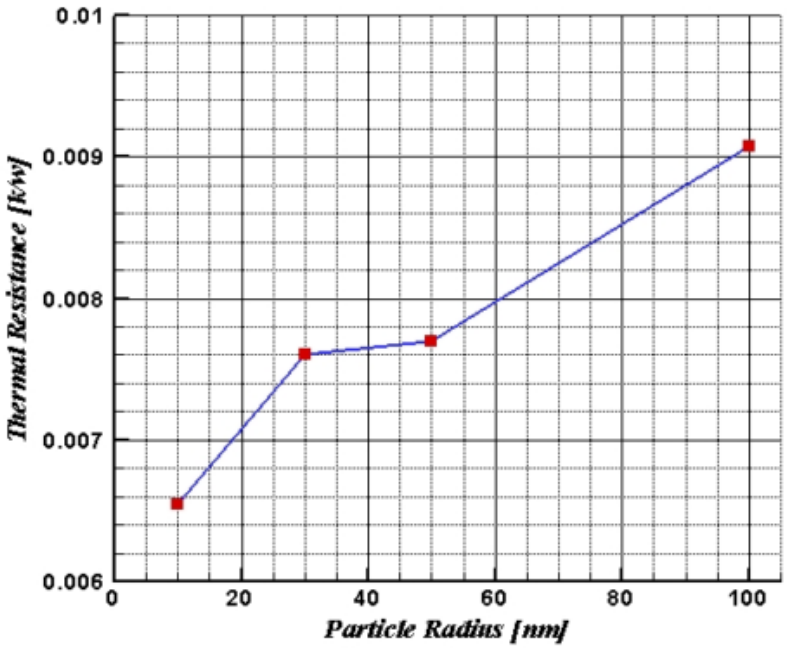

Figure 2.3 Relationship between heated pipe thermal resistance with nanoparticle radius(Gavtash et al., 2012)

2.4 Nanofluids Thermophysical

(Asirvatham et al. 2009) have presented an experimental study of steady state convective heat transfer of de-ionized water with a low volume fraction (0.003% by volume) of copper oxide (CuO) nanoparticles dispersed to form a nanofluid that flows through a copper tube. The effect of mass flow rate ranging from (0.0113 kg/s to 0.0139 kg/s) and the effect of inlet temperatures at 10 ^{o}C and 17 ^{o}C on the heat transfer coefficient are studied on the entry region under laminar flow condition. The results have shown 8% enhancement of the convective heat transfer coefficient of the nanofluid even with a low volume concentration of CuO nanoparticles. The heat transfer enhancement was increased considerably as the Reynolds number increased. Possible

reasons for the enhancement are discussed. Nanofluid thermo-physical properties and chaotic movement of ultrafine particles which accelerate the energy exchange process are proposed to be the main reasons for the observed heat transfer enhancement.

(Bayat & Nikseresht 2012) numerically studied the enhancement of nanofluids convective heat transfer through a circular tube with a constant heat flux condition in the turbulent flow regime. The incompressible and steady-state forms of continuity, Navier Stokes and energy equations have been solved using finite volume approach with the SIMPLER algorithm. From the results, it can be deduced that for a fixed Reynolds number, increasing the particle concentration enhances convective heat transfer rate considerably. Moreover, there was a large pressure drop and pumping power when using nanofluids instead of base fluid with the same Reynolds number.

(Ko et al. 2007) reported an experimental study on the flow characteristics of the aqueous suspensions of carbon nanotubes (CNTs) in his article. The pressure drops in a horizontal tube and viscosities of nanofluids were measured and the effects of CNT loading and different preparation methods were investigated. Viscosity measurements show that both CNT nanofluids prepared by two methods are shear thinning fluids and at the same volume fraction, the nanofluids prepared by the acid treatment have much smaller viscosity than the ones made with surfactant. Under laminar flow conditions, the friction factor of CNT nanofluids stabilized by adding surfactant is much larger than that of CNT nanofluids prepared by acid treatment, and both nanofluids show larger friction factors than distilled water. In contrast to this, under turbulent flow conditions, the friction factors of both nanofluids become similar to that of the base fluids as the flow rate increases. It was also shows that as CNT loading is increased, laminar regime of nanofluids has been extended to further higher flow rates, therefore, nanofluids could have low friction factors than pure water flows at certain range of flow rates.

(Liu et al. 2011) investigated the enhancements of thermal conductivities of ethylene glycol, water, and synthetic engine oil in the presence of copper (Cu), copper oxide (CuO), and multi-walled carbon nanotube (MWNT) using both physical mixing method (two-step method) and chemical reduction method (one-step method). Experimental results show that nanofluids with low concentration of Cu, CuO, or carbon nanotube (CNT) have considerably higher thermal conductivity than identical base liquids. For CuO-ethylene glycol suspensions at 5 vol.%, MWNT-ethylene glycol at 1 vol.%, MWNT-water at 1.5 vol.%, and MWNT-synthetic engine oil at 2 vol.%, thermal conductivity was enhanced by 22.4, 12.4, 17, and 30%, respectively. For Cu-water at 0.1 vol.%, thermal conductivity was increased by 23.8%. The thermal conductivity improvement for CuO and CNT nanofluids was approximately linear with the volume fraction. This result clearly indicates that the enhancement of cooling capacity is not just related to thermal conductivity alone. Dynamic effect, such as nanoparticle dispersion may effectively augment the system performance. They were also found that the dynamic dispersion is comparatively effective at lower flow rate regime, e.g., transition or laminar flow and becomes less effective at higher flow rate regime. Test results show that the coefficient of performance of the water chiller is increased by 5.15% relative to that without nanofluid.

2.5 Numerical Investigation of Annular Pipe

(Zeinali Heris et al. 2007) was investigated experimentally the laminar flow forced convection heat transfer of Al_2O_3/water nanofluid inside a circular tube with constant wall temperature. The experimental results emphasize the enhancement of heat transfer due to the nanoparticles presence in the fluid. Heat transfer coefficient increases by increasing the concentration of nanoparticles in nanofluid. The increase in heat transfer coefficient due to presence of nanoparticles is much higher than the prediction of single phase heat transfer correlation used with nanofluid properties.

(Togun et al. 2011) experimentally studied the effect of step height on heat transfer to a radially outward expanded air flow stream in a concentric annular passage. Separation, subsequent reattachment and developed air flow occurred in the test section at a constant heat flux boundary condition. The investigation was performed in a Re range of 17050–44545, heat flux varied from 719 W/m^2 to 2098 W/m^2 and the enhancement of step heights were, s = 0 (without step), 6 mm, 14.5mmand 18.5 mm, which refer to d/D = 1, 1.16, 1.53 and 1.80, respectively. For all cases, an increase in the local heat transfer coefficient was obtained against enhanced heat flux and or Re. The effect of step variation is prominent in heat transfer at the separation region which increases with the rise of step height and it shows a little effect in the redevelopment region. In the separation region, the local heat transfer coefficient increases up to the maximum value at the reattachment point and then decreases gradually in the redevelopment region.

(Bianco et al. 2011) numerically analyzed the turbulent forced convection flow of water/Al_2O_3 nanofluid in a circular tube, subjected to a constant and uniform heat flux at the wall. Two different approaches are taken into account: single and two-phase models, with particle diameter equal to 38 nm. He was observed that convective heat transfer coefficient for nanofluids is greater than that of the base liquid. Heat transfer enhancement increases with the particle volume concentration and Reynolds number. Comparisons with correlations present in literature are accomplished and a very good agreement is realized.

(Fotukian & Nasr Esfahany 2010) investigated experimentally the turbulent convective heat transfer and pressure drop of c-Al_2O_3/water nanofluid inside a circular tube. The volume fraction of nanoparticles in base fluid was less than 0.2%. Results indicated that addition of small amounts of nanoparticles to the base fluid augmented

heat transfer remarkably. Increasing the volume fraction of nanoparticles in the range studied in this work did not show much effect on heat transfer enhancement. Measurements showed that pressure drop for the dilute nanofluid was much greater than that of the base fluid. Experimental results were compared with existing correlations for nanofluid convective heat transfer coefficient in turbulent regime.

(Kumar & Dhiman 2012) investigated the augmentation in the laminar forced convection characteristics of the backward-facing step flow in a two-dimensional channel by means of introducing an adiabatic circular cylinder in the domain. The effects of various cross-stream positions of the circular cylinder on the flow and heat transfer characteristics of the backward-facing step flow has been numerically explored for the Reynolds number range 1e200 and Prandtl number of 0.71 (air). The results showed an enhancement in the peak Nusselt value of up to 155% using a circular cylinder as compared to the unobstructed case (i.e., without cylinder).

CHAPTER 3: METHODOLOGY

3.1 Model configuration

The considered geometrical configuration for this study shown in Figure 3.1. The schematic diagram was first designed using DesignModeler in ANSYS Workbench based on research done by (Togun et al. 2011) . Due to the symmetrical shape of the model, the used of 2D axisymmetric design have been applied to the system. The ratio of downstream channel height, *H* to the inflow channel height,*h*. known as an expansion ratio (ER) is set to be 2.5, 1.8 and 1.2 for simulation of CuO/water and constant at *ER*=1.8 for the other nanofluids considered in this study. The heated pipe area was considered as a test section in the current study. The length of heated pipe is 0.6m and length of unheated pipe is 0.5m. The entrance pipe diameter is varies depends on step height and the test pipe diameter is 83mm. The inner tube with diameter of 22mm used to produce an annular geometry to the pipe.

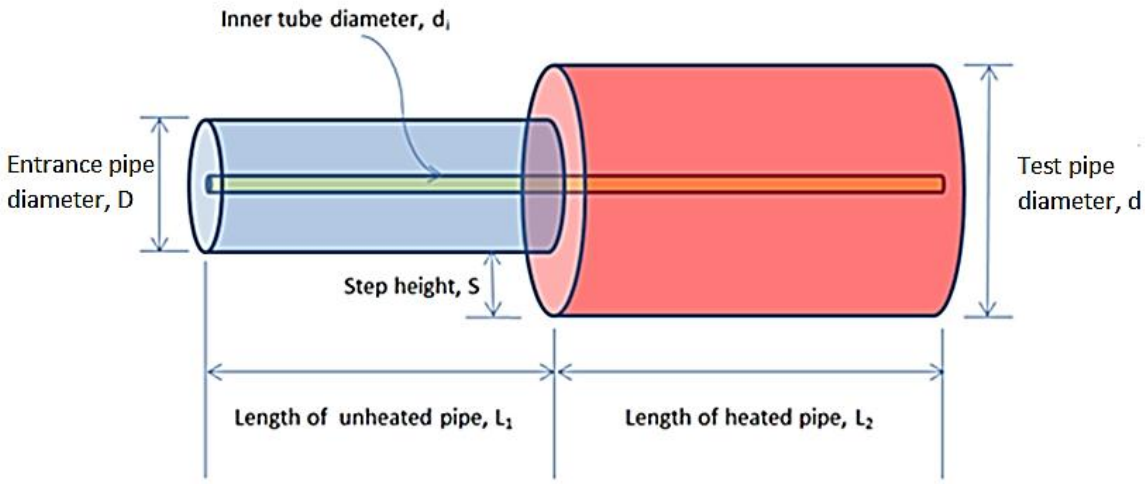

Figure 3.1: Schematic diagram of annular pipe in sudden expansion

The 2D model of the pipe for CFD simulation, shown in Figure 3.2. In this study, the standard step height, S = 13.5mm was used for all the running simulations,

except for CuO/water which varies with a step height of 18.5mm, 13.5mm and 6.0mm. The test pipe at length of 0.6m is heated with uniform heat flux, *q* along the test section. To attain a fully developed turbulent flow enter the entrance of test tube, the unheated pipe have been divided into three interiors. The velocity of fluid flow through each interior, will be compared with the heated pipe entrance velocity. The constant value of velocity will verify the condition of fully developed turbulent flow in a test section.

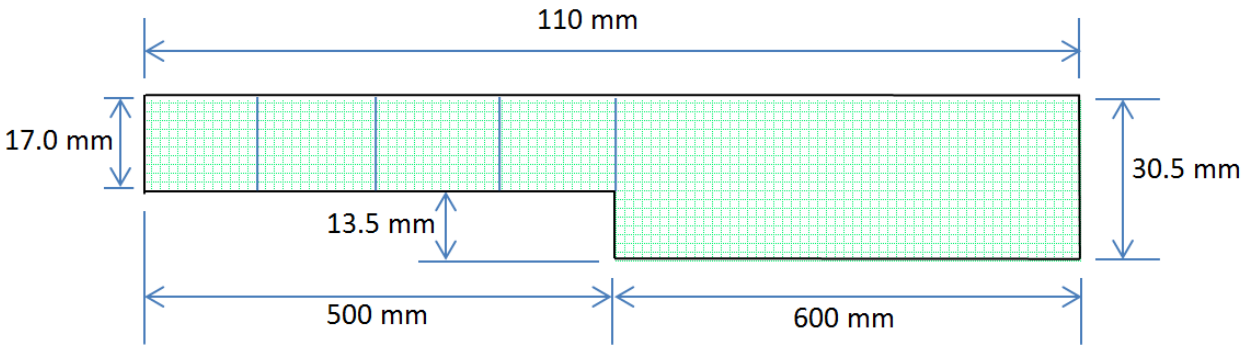

Figure 3.2: The 2D model of the pipe for CFD simulation(step height, S=13.5mm)

3.2 Thermophysical properties of nanofluids

The thermophysical of CuO-water, Al_2O_3-water and TiO_2-water nanofluids has been scrutinized by using mathematical formulation to compare the heat transfer performance of the respective nanofluids. The heated annular tube operation is analyzed with the nanofluids serve as a working fluid. Thermophysical properties of the water and nanoparticles (CuO, Al_2O_3 and TiO_2) shown in Table 3.1(Saffari Pour 2012).

Table 3.1: The properties of the water and nanoparticles

Fluid/Nanoparticles	Properties			
	ρ(kg/m^3)	μ(N.s/m^3)	Cp(J/kg.K)	k(W/m.K)
H_2O	997.1	724.6 x 10^{-6}	4179	0.613
CuO	6500	-	535.6	20
Al_2O_3	3970	-	765	40
TiO_2	4250		686.2	8.9538

The volume fraction(φ) of nanoparticles inside the base fluids gave a different thermophysical value of nanofluids (Sureshkumar et al. 2013). The properties were determined using Eq.(12) to Eq.(15). Nanoparticle shape factor (n) assumed to be 3 for spherical particles. The current study will analyze and compare the performance of three nanofluids consist of 2.0% volume fraction of the fluids particles, except for Al_2O_3/water which also simulated with 0.5% and 1.0% particles concentration . With the same model description, variations also implicate four values of Reynolds number for each nanofluids. The calculated properties of nanofluids shown in Table 3.2 below for 2% particles concentration.

Table 3.2: Thermophysical properties of nanofluids(for volume fraction $\boldsymbol{\varphi}$**=2%)**

Nanofluids	**Properties**			
	ρ(kg/m^3)	**μ(N.s/m^3)**	**Cp(J/kg.K)**	**k(W/m.K)**
CuO/Water	1107.158	0.000761	3751.2	0.661281
Al_2O_3/Water	1056.558	0.000761	3922.439	0.648824
TiO_2/Water	1062.158	0.000761	3899.486	0.643638

3.3 Governing equations and parameters

In this study, fully developed turbulent flow will be investigated numerically. A few equations involved in determining exact solutions for heat transfer performance of nanofluids flowing through an expansion of annular heated pipe. The uniformly subjected heat flux at the test section will transfer the heat to the fluids by force convection and the equations utilize for this investigation will be discuss further in this section.

The Reynolds number for the nanofluids was computed based on the inlet bulk velocity U and the distance,x by using the following equation, Eq.(16):

$$Re_x = \frac{\rho_{nf} U x}{\mu_{nf}} \tag{16}$$

where U is the fluid velocity, ρ is the fluid density, μ is the dynamic viscosity of the fluid. The subscript *nf* stand for nanofluid properties.

By using the simulated data from numerical analysis, the convective heat transfer coefficient can be calculated as :

$$h_{nf} = \frac{q''}{(T_s - T_b)} \tag{17}$$

where q'' is the heat flux supplied by the heaters at the test area, T_s is the average surface temperature and T_b is the average of fluid inlet and outlet temperature. The heat flux is derived from $\dot{q}$, the rate of heat gained by the fluid flowing through the test section, which is given as:

$$\dot{q} = \dot{m} C_p \Delta T_f \tag{18}$$

where $\dot{m}$ is the mass flow rate, C_p is the specific heat of nanofluid and ΔT_f is the difference between outlet and inlet temperatures of the nanofluid. Dividing the heat transfer rate by the inside surface area of the tube, the heat flux is obtained.

The value of T_b can be found using the following equation:

$$T_b = \frac{\left(T_{out,avg} - T_{in,avg}\right)}{2} \tag{19}$$

where $T_{out,avg}$ and $T_{in,avg}$ assigned for average outlet and inlet temperature (Assume at the room temperature, 300K).

The thermal parameter Nusselt number (Nu_x) based on distance is estimated using Eq.(20):

$$Nu_x = \frac{h_{nf} \cdot x}{k_{nf}} \tag{20}$$

where x is the distance and k_{nf} is the thermal conductivity for the nanofluids. The relation of Nusselt number (*Nu*) with Reynolds(*Re*) and Prandtl (*Pr*) number for fully developed turbulent flow shown below (Maïga et al. 2006):

$$Nu_{fd} = 0.085Re^{0.71}Pr^{0.35} \tag{21}$$

In a fully developed pipe flow, the turbulent length scale(*l)* can be estimated as 7% of hydraulic diameter (D_h) (CFD-Online), as in Eq.(22):

$$l = 0.07D_h \tag{22}$$

The value of hydraulic diameter can be computed from the following equation.

$$D_h = 2\frac{L \cdot w}{L + w} \tag{23}$$

Where *L* and *w* is a length and width of the passage.

The most popular computer model used to solve complicated turbulent model analytically is $k - \varepsilon$ model(Stolpa 2004). The definition of k, the turbulent energy, is:

$$k = \frac{1}{2}\left[\overline{(u')^2} + \overline{(v')^2} + \overline{(w')^2}\right] \tag{24}$$

The dissipation rate(ε) is defined as:

$$\varepsilon = C_D\frac{k^{3/2}}{l} \tag{25}$$

where C_D is a constant and l is a yet to be determined length scale similar to the mixing length.

3.4 Boundary properties

The schematic diagram of boundary condition shows in Figure 3.3. The pipe inlet is a fully developed turbulent flow with the maximum streamwise velocity of U_∞.

The fluid was allowed to flow freely leaving the outlet with minimum consideration(Prasad V.Tota 2009). The part in contact with the inner tube is a symmetry free slip boundary while the cylindrical pipe wall (y=0) is a no slip viscous wall. The test section is assigned as a wall in meshing part, but then defined as heat flux in FLUENT for numerical analysis.

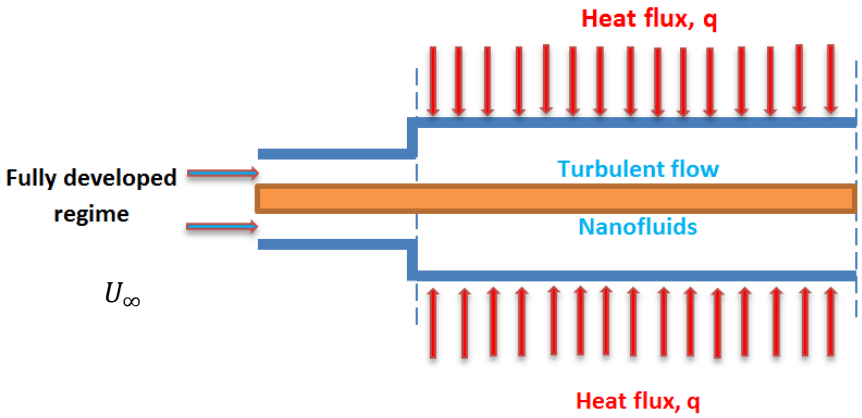

Figure 3.3: Schematic boundary condition for the pipe

All the boundary and edges are defined in DesignModeler in order to justify the condition for each part. Table 3.3 specify the types of boundary that being assigned for each edges. To meet the requirement of velocity-pressure coupling for k-ε equation in FLUENT, the inlet and outlet are defined as velocity inlet and pressure outlet.

Table 3.3: Boundary type for all the edges

Edge	**Type of Boundary**
Inlet	Velocity Inlet
Interior 1	Interior
Interior 2	Interior
Interior 3	Interior
Step	Wall
Heated Wall	Wall
Outlet	Pressure Outlet

The division of interiors caused the separation of the model into five faces, as shown in Figure 3.4a. The mesh element Quad with the type Map was used to mesh all the faces. The mesh interval size 6 used in this study and generate 2887 number of nodes with 836 elements(Figure 3.4b). The next process is to simulate using FLUENT for the numerical analysis.

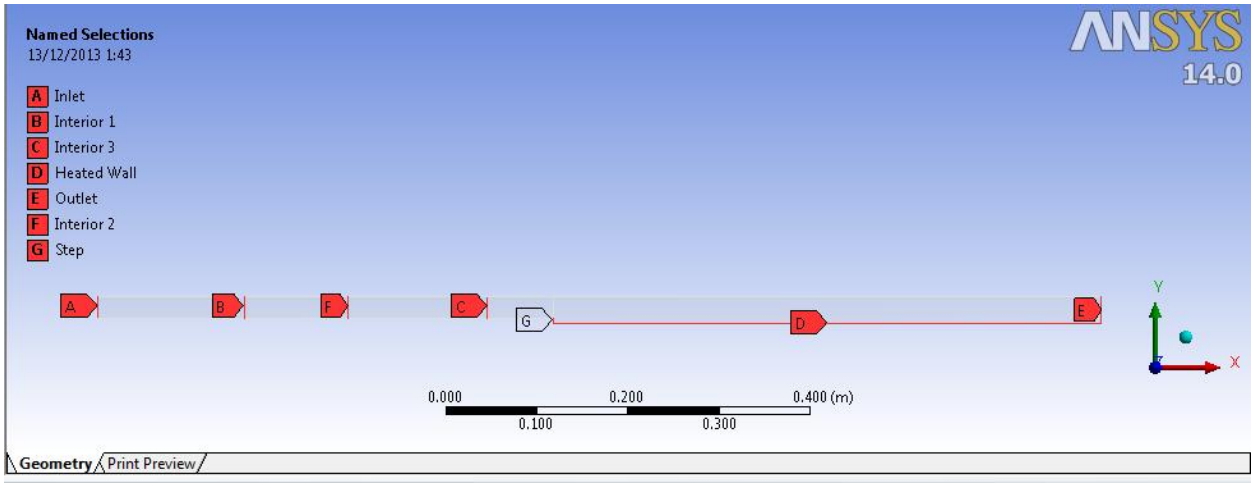

(a)

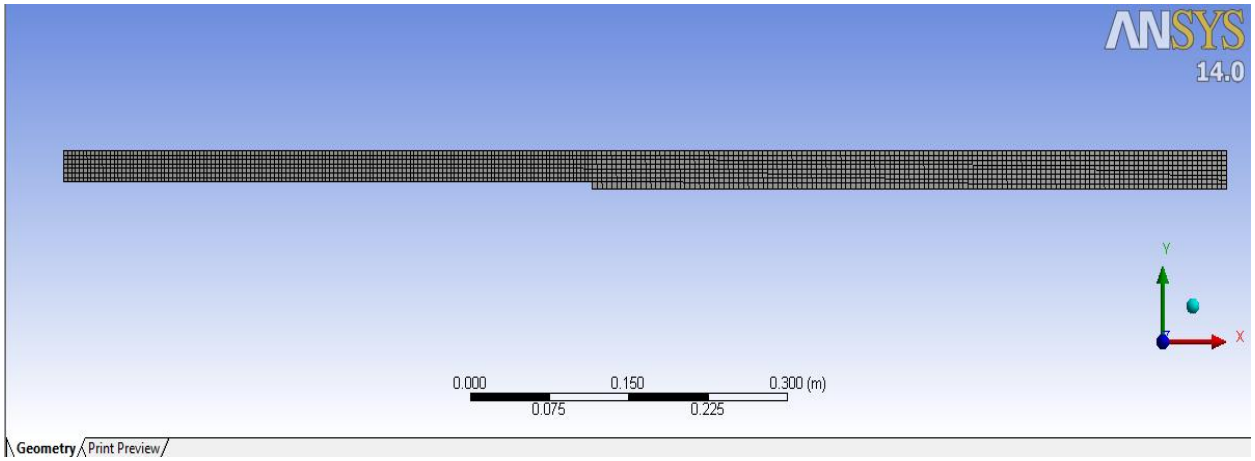

(b)

Figure 3.4: a) Label of boundary type for the edges, b) Model meshed with Quad element type Map

3.5 Numerical simulations

The analysis of fluid flow and heat transfer inside heated pipe is a very complex process. There are many factors associated with the efficiency of a thermal CFD simulation. The appropriate justification of model description, mesh generation, numerical computing scheme, and integration of physical domain will lead to the successful of numerical simulation process. The computational simulation for the backward facing step of annular passage was utilized by using ANSYS Fluent-14.0, which is fully integrated with fluid analysis software of ANSYS Workbench platform. This software combines CAD modeling using DesignModeler, complex meshing solution, fast solution algorithm and post-processing facilities.

This study investigated the performance of three types of nanofluids in fully developed unsteady turbulent flow. Each nanofluids are tested with four different value of Reynolds number: *Re* = 17050, 30720, 39992 and 44545. The contour of velocity profile from the simulation will assured that turbulent flow enter the entrance of test section. Uniform heat flux applied on the heated pipe wall with the value of 49050 W/m^2, based on research by (Saeedinia et al. 2012). To solve for turbulent flow, the pressure based solver with 2^{nd} order implicit unsteady formulation applied with standard k-epsilon equation. The SIMPLE algorithm used to establish the coupling of pressure and velocity. For higher order differencing scheme, this algorithm compromises better efficiency of coupled parameters iteration. By using SIMPLE algorithm, the mass conservation and momentum equation are linked together through pressure correction.

The thermophysical properties of the nanofluids material were used in this simulation by uploading the data inside Fluent material database, as shown in Figure 3.5 below. The simulation of the backward facing step model able to use it directly, once the data have been created. The boundary condition for the outlet is defined as pressure

outlet with turbulent length scale 0.02m and turbulent intensity 7%. The computational conditions for simulation in Fluent shows in Table 3.4 below.

The pure water is used as the working fluid before the evaluation of heat transfer characteristic of the nanofluids inside annular heated pipe. It is used to estimate the accuracy of numerical analysis model. In order to validate the numerical analysis model from this study, results will be compared with the experimental results.

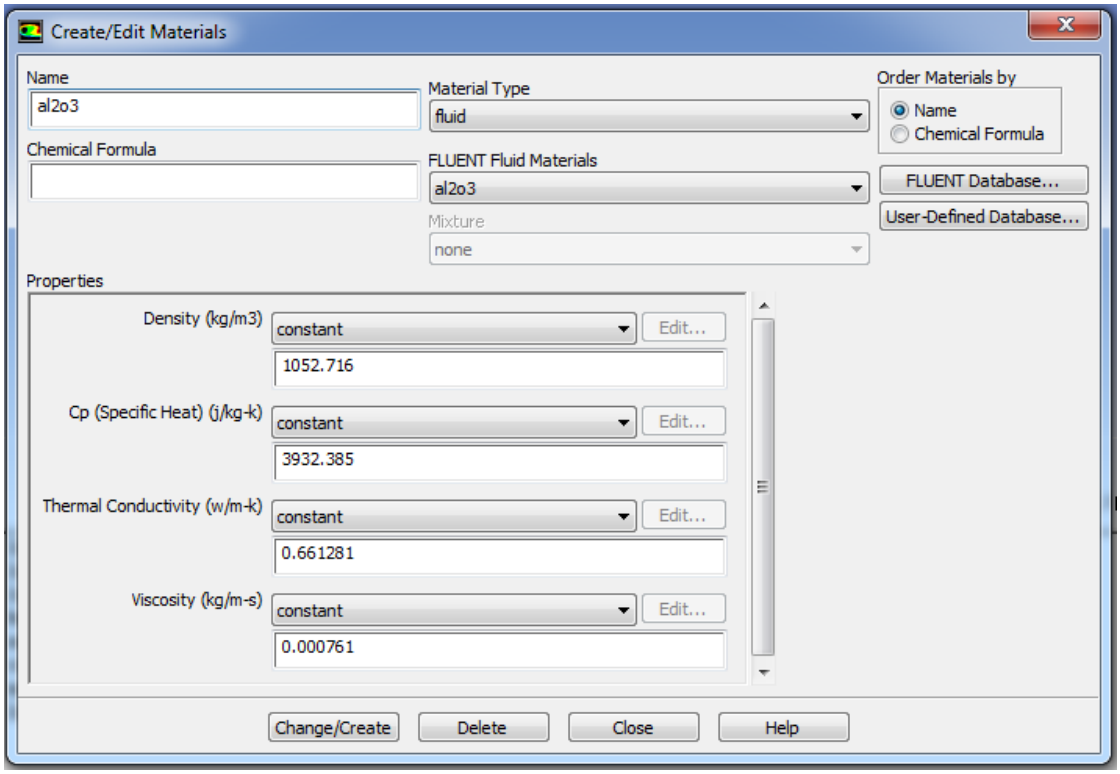

Figure 3.5: Material database in FLUENT

Table 3.4: Computational simulation properties in FLUENT

Pressure-Velocity Coupling	SIMPLE	**Maximum X**	1.1m
Discretization (momentum)	2nd Order Upwind	**Maximum Y**	0.0305 m
Discretization (turbulence)	2nd Order Upwind	**Inlet boundary type**	Velocity Inlet
Viscous model	k-epsilon, standard	**Outlet boundary type**	Pressure Outlet
Space/Time	2D/Unsteady 2nd Order Implicit	**Iteration time step**	0.1s
Residual error	1×10^{-4}	**Number of time steps**	100

CHAPTER 4:RESULT AND DISCUSSION

In this study, the nanofluids of CuO and TiO_2 with 2% particle concentration and 0.5%, 1% and 2% of Al_2O_3 volume fraction with the base fluid water have been compared in terms of their heat transfer performances. Numerical investigation for sudden expansion of annular passage with three step height, S=6, 13.5 and 18.5mm for CuO/water simulation and constant step height of 13.5mm for Al_2O_3 and TiO_2 were carried out. The variation of Reynolds number, *Re* = 17050, 30720, 39992, and 44545 have produced a turbulent flow with various value of fluid velocity inside the annular passage which heated uniformly with constant heat flux of 49050 W/m^2.

4.1 Velocity distribution

This section will discuss the fluid flow at turbulent Reynolds number, *Re* = 17050, 30720, 39992, and 44545 for various type of nanofluids. The flow velocity is influenced by thermophysical properties of nanofluids used. Based on Eq.(16), Table 4.1 shows the variations of inlet velocity for each nanofluid at 2% volume fraction. All nanofluids are found to flow with velocity less than 2 m/s in order to achieve the respective Reynolds number. Alumina(Al_2O_3) is initiated to flow with the highest velocity at 1.8873m/s for the highest Reynolds number.

Table 4.1: Variations of inlet velocity for the nanofluids (volume fraction=2%)

Reynolds No	Velocity(m/s)			
	CuO/Water	Al_2O_3/Water	TiO_2/Water	Water
17050	0.6894	0.7224	0.7186	0.7292
30720	1.2421	1.3016	1.2947	1.3139
39992	1.6170	1.6944	1.6855	1.7105
44545	1.8010	1.8873	1.8774	1.9052

Based on Figure 4.1, the variations of velocity shows that copper oxide(CuO) flow in less velocity compared to others for the respective Reynolds number. The pattern of velocity distribution is compared with the water to verify the investigation. The hydraulic diameter consider in this study is the same as inlet diameter of the fluids which is, D_h=0.017m for step height 13.5mm and D_h=0.024 and 0.012m for the other step heights.

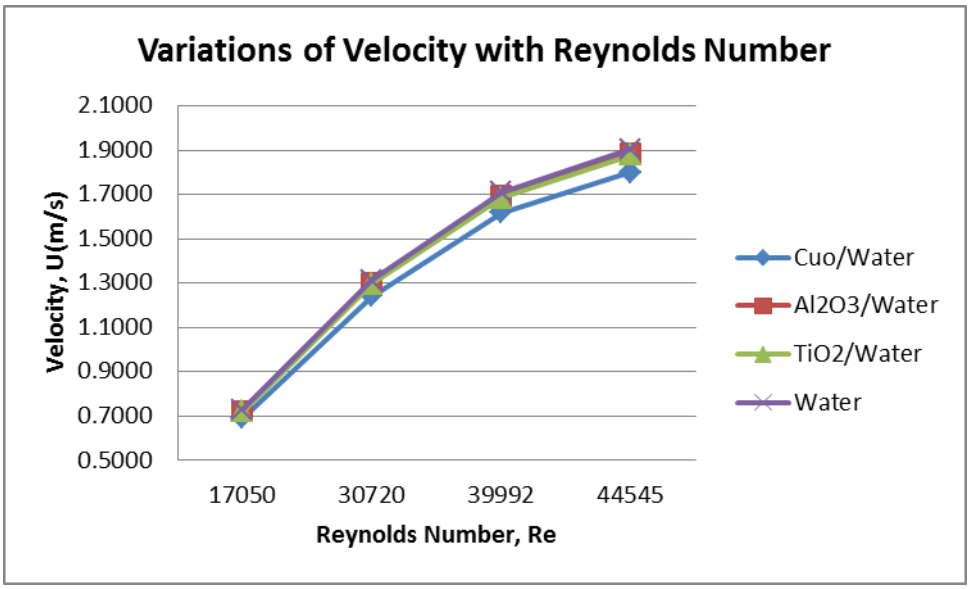

Figure 4.1: Variations of velocity with Reynolds number(at 2% volume fraction)

Figure 4.2 shows the velocity vector distribution for alumina(Al_2O_3). The figures shows the color variations from blue to red due to the amount of velocity for each cases. The vector of fluid flow passes the unheated pipe with fully developed turbulent flow and enter the inlet of heated pipe with the same velocity as at entrance.

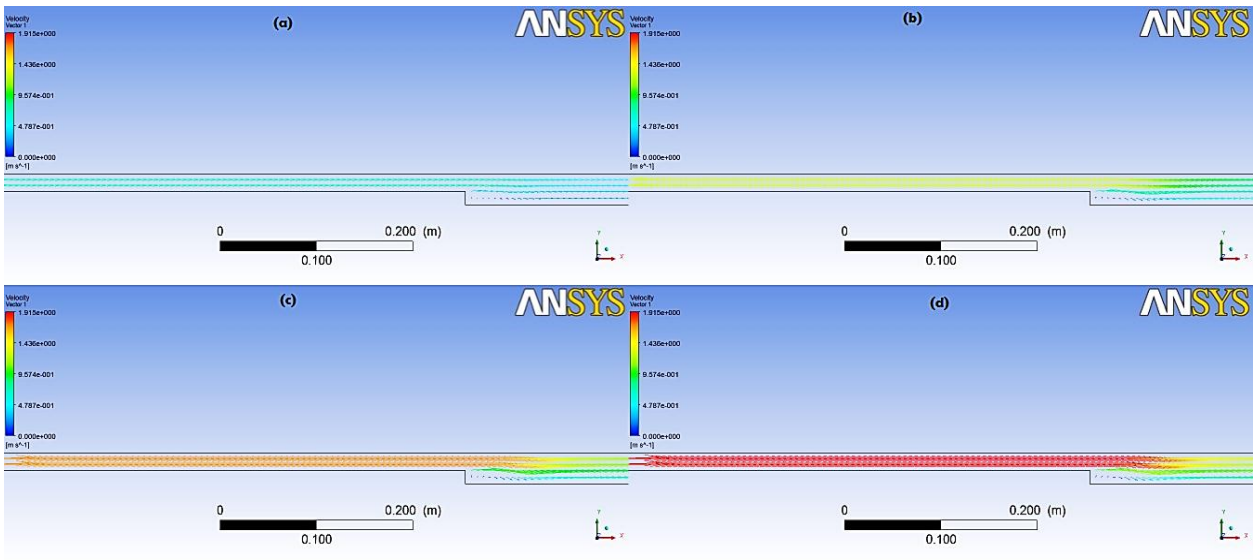

Figure 4.2: Velocity vector distribution for Al_2O_3/Water at a)*Re*=17050, b)*Re*=37020, c)*Re*=39992 and d) *Re*=44545

4.2 Analysis of Various Local Surface Temperature

Figure 4.3 shows the variations of temperature with pipe distance for water, as a benchmark to verify the model. The range of temperature fall between 300K to 325K with the lowest temperature occur at *x*=0.542m for each Reynolds number. Higher Reynolds number turn to produce less temperature distribution compared to others for water. The minimum temperature for water flow at *R*e=17050,*Re*=30720, *Re*=39992 and *Re*=44545 are T=306.07K, 303.43K, 302.66K and 302.4K. This findings shows that minimum temperature occur at the reattachment length for the highest Reynolds number of water.

Figure 4.4 shows the variations temperature for alumina/water with the pipe distance. The pattern shows the reduction of temperature at the reattachment point just after the step for the same model at *x*=0.542m in terms of the step height. The value of minimum temperature,T for each Reynolds number are 305.9K, 303.35K, 302.59K and 302.33K.

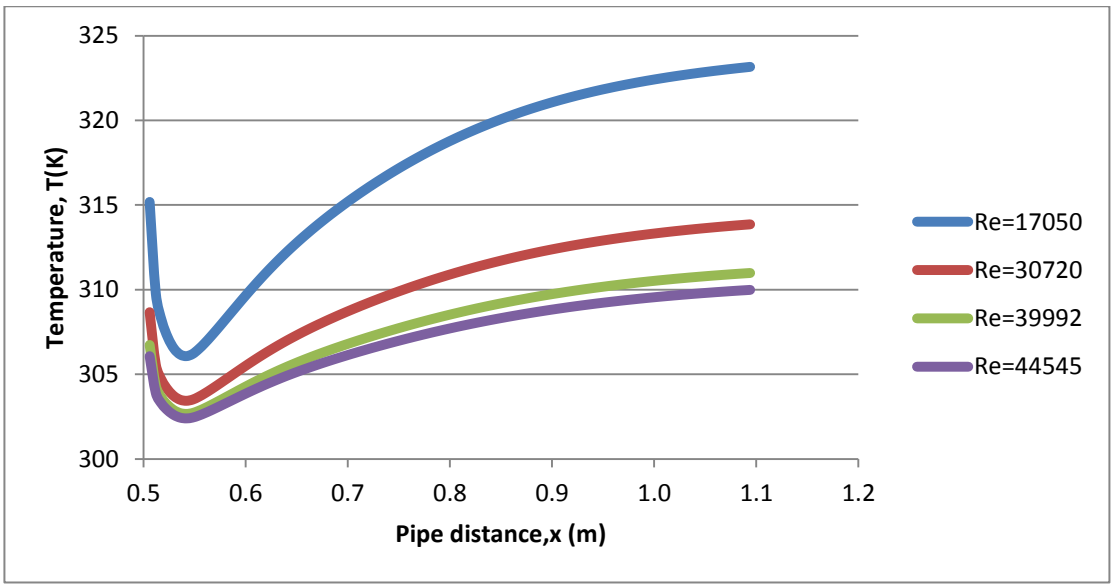

Figure 4.3: The variations of temperature with pipe distance for water

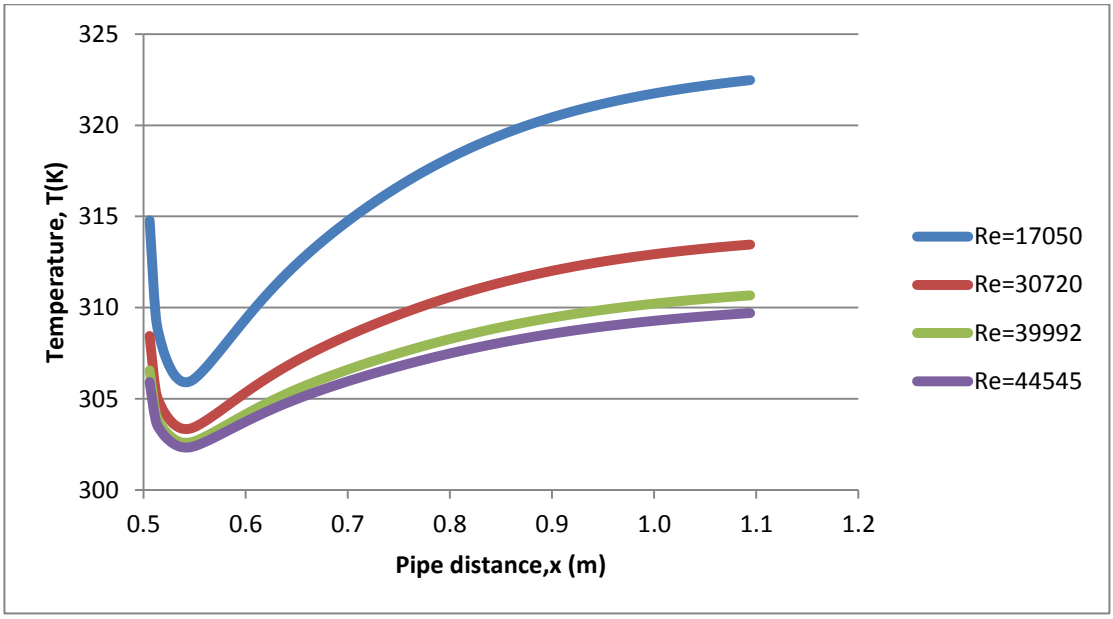

Figure 4.4: The variations of temperature with pipe distance for Al_2O_3/water

Figure 4.5 shows the variations of temperature with pipe distance for copper dioxide, CuO/water. The lowest temperature occur at the same position like other nanofluids which is at x=0.542m. The minimum temperature for CuO/Water at the respective Reynolds number are T=303.4K, 305.96K, 302.61K and 302.36K. Higher

Reynolds number produced less temperature distribution compared to lower Reynolds number.

Figure 4.6 the variations temperature for titanium dioxide,TiO_2/water with the pipe distance have been presented. The general pattern shows the reduction of temperature at the reattachment point just after the entrance of heated pipe, at x=0.542m. The value of minimum temperature,T for each Reynolds number are 305.95K, 303.37K, 302.61K and 302.35K.

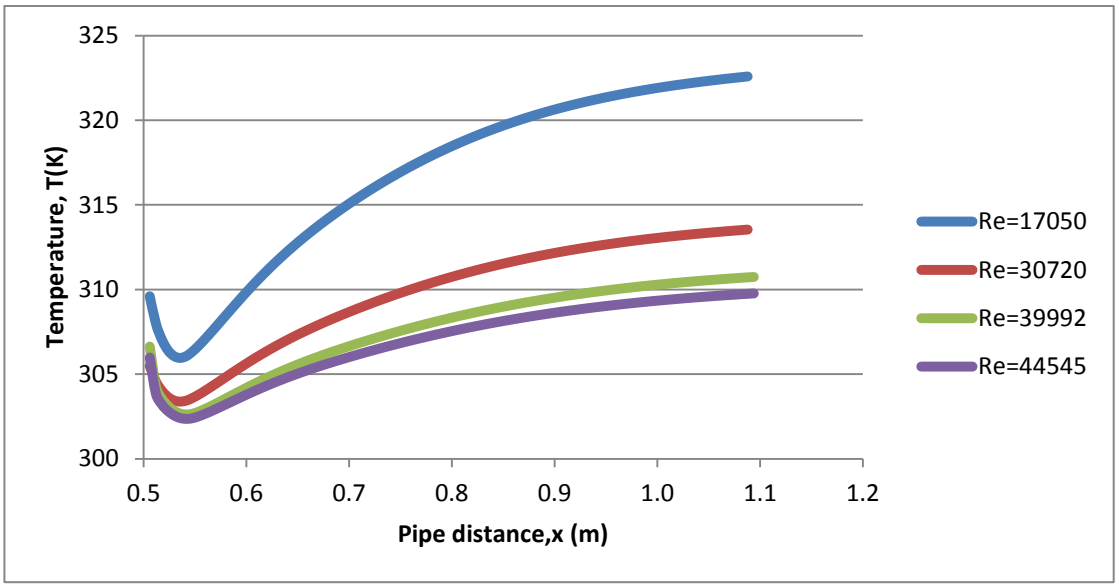

Figure 4.5: The variations of temperature with pipe distance for CuO/water

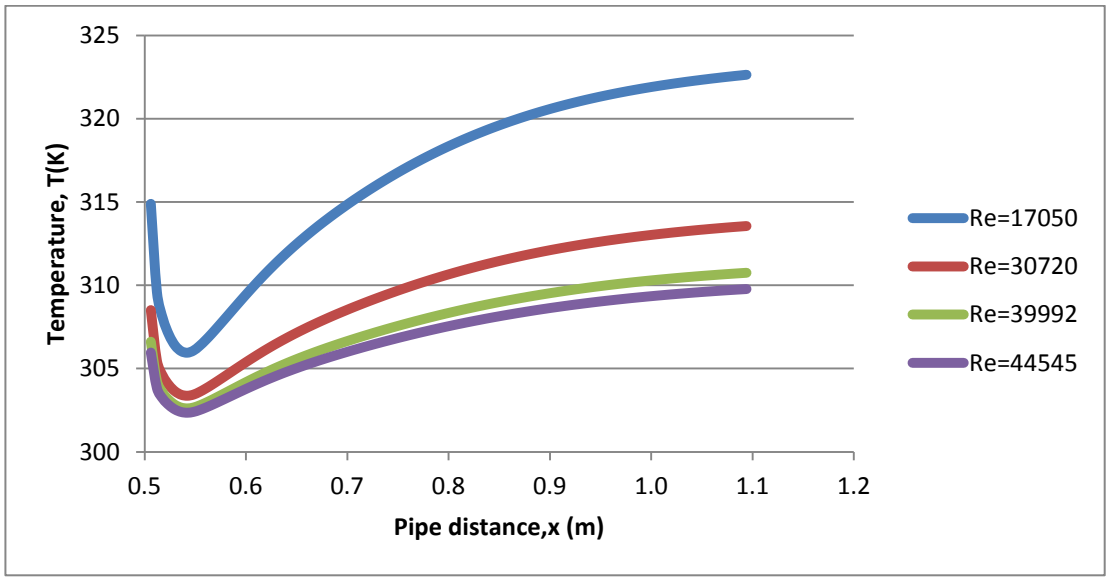

Figure 4.6: The variations of temperature with pipe distance for TiO_2/water

4.3 Temperature Distribution Based on Reynolds Number

The temperature distribution for all the working fluids at Reynolds number 17050 is illustrated in Figure 4.7 for 2% volume fraction and step height 13.5mm. The graph present less temperature after the steps for all nanofluids at this turbulent mode . All the nanofluids, seem to be close with water temperature distribution pattern for the constant heat flux, q=49050 W/m^2. The temperature profile shows the sharp decrement after the step and gradually increases for all the working fluids along the test pipe. The lowest temperature found at 0.542m after the step for Al_2O_3 , at T=305.91K. The data shows that by using nanofluids at *Re*= 17050, the average temperature distributions is about 0.14% below the water which is approximately 316K.

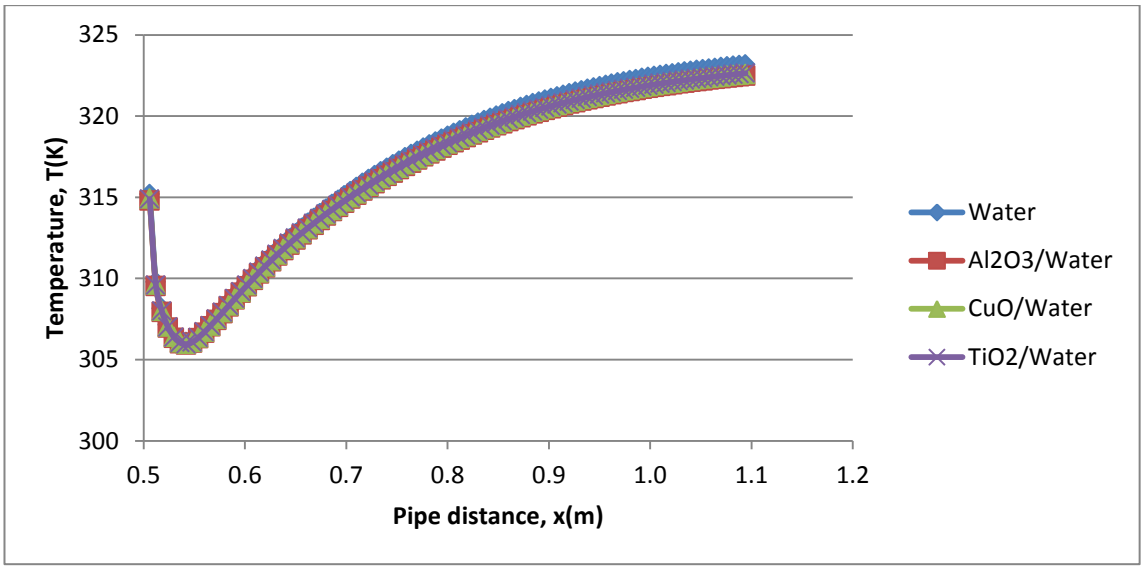

Figure 4.7: Temperature variations for water and nanofluids at Re=17050

The variations of surface temperature for Reynolds number of 37020 plotted in Figure 4.8. The distribution is just the same for all the working fluids, which having the same heat flux and step height. The result shows the increment of surface temperature enhancement along the heated pipe after the flow reattachment point. The average temperature found to be 309K, and the lowest temperature occur at T=303.3K for Al_2O_3.

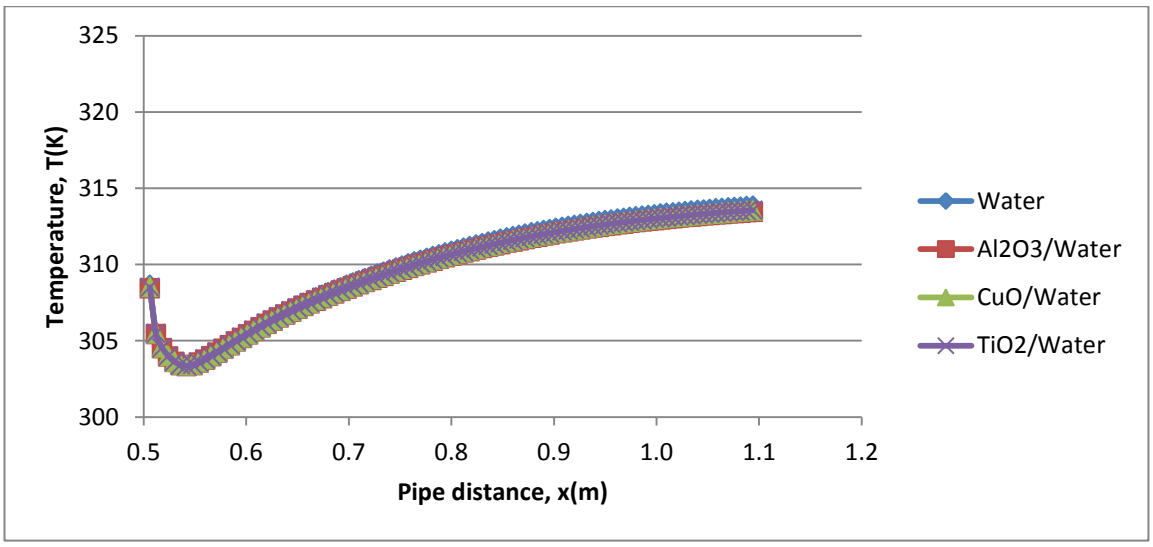

Figure 4.8: Temperature variations for water and nanofluids at Re=30720

The temperature variations for Re=39992 and Re=44545 shown in Figure 4.9 and Figure 4.10. The result shows that all the working fluids have the same pattern of surface temperature on the heated pipe. For the same model of annular passage, with higher Reynolds number, the variations of temperature along the test pipe observed to have the significant value with slight different of 0.1% . The average temperature distribution for Re=39992 is 307K and for Re=44545 is 306K. The average temperature was drop as the Reynolds number increase for all the nanofluids.

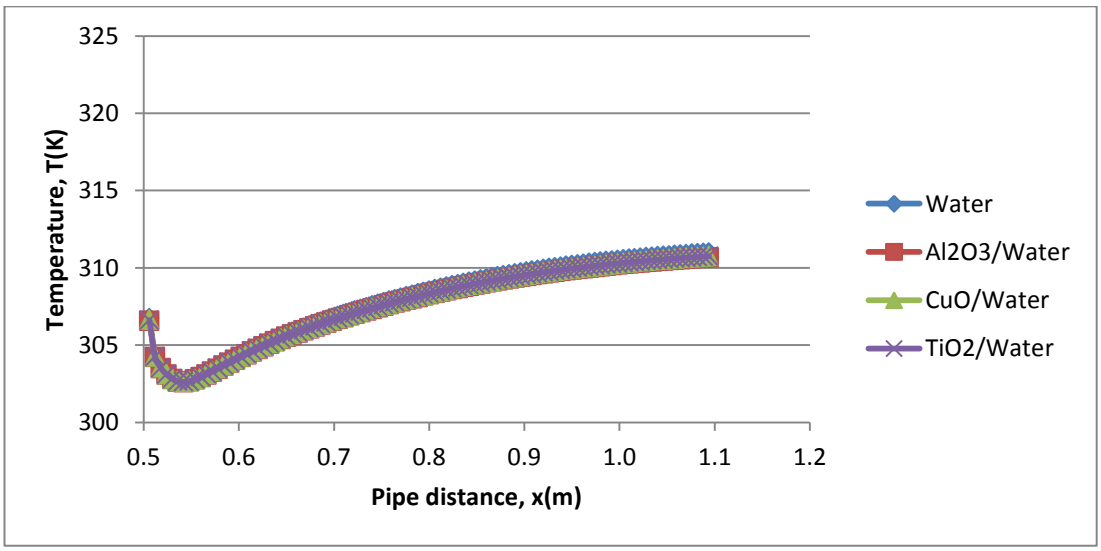

Figure 4.9: Temperature variations for water and nanofluids at Re=39992

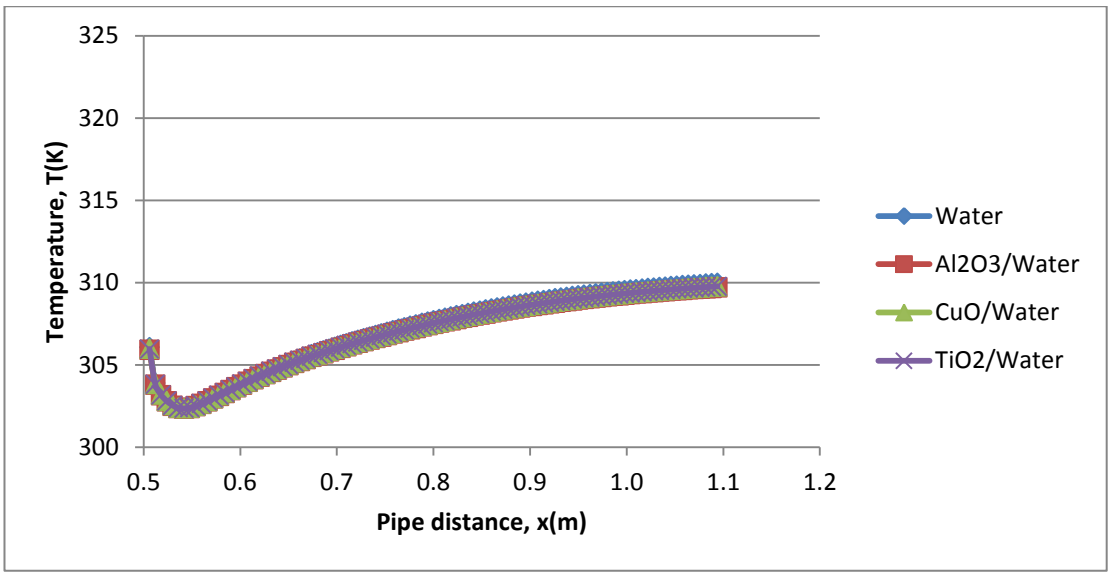

Figure 4.10: Temperature variations for water and nanofluids at Re=44545

4.4 Evaluation of Heat Transfer Rate

The volume fraction of nanoparticle influences the heat transfer characteristics of nanofluids. This behavior is due to their differing thermophysical properties. The three metallic particles CuO, TiO_2 and Al_2O_3 have higher density, higher thermal conductivity and produce more viscous nanofluid compared to other non-metallic particle. Because of the higher values of the properties of the metallic particles, the nanofluids containing them generate higher heat transfer coefficients than the non-metallic particle.

At a Reynolds number of 17050 the heat transfer coefficient for all the working fluids generate the same pattern over the water, as shown in Figure 4.11. The combined effects of these particle properties play the role in enhancing the heat transfer coefficient of nanofluids. The value of heat transfer rate sharply decrease after the reattachment point at x=0.542m and keep decreasing until the outlet. The highest heat transfer coefficient occur at the reattachment point of Al_2O_3 at 16595 W/m^{2}K for constant heat flux and volume fraction of 2%.

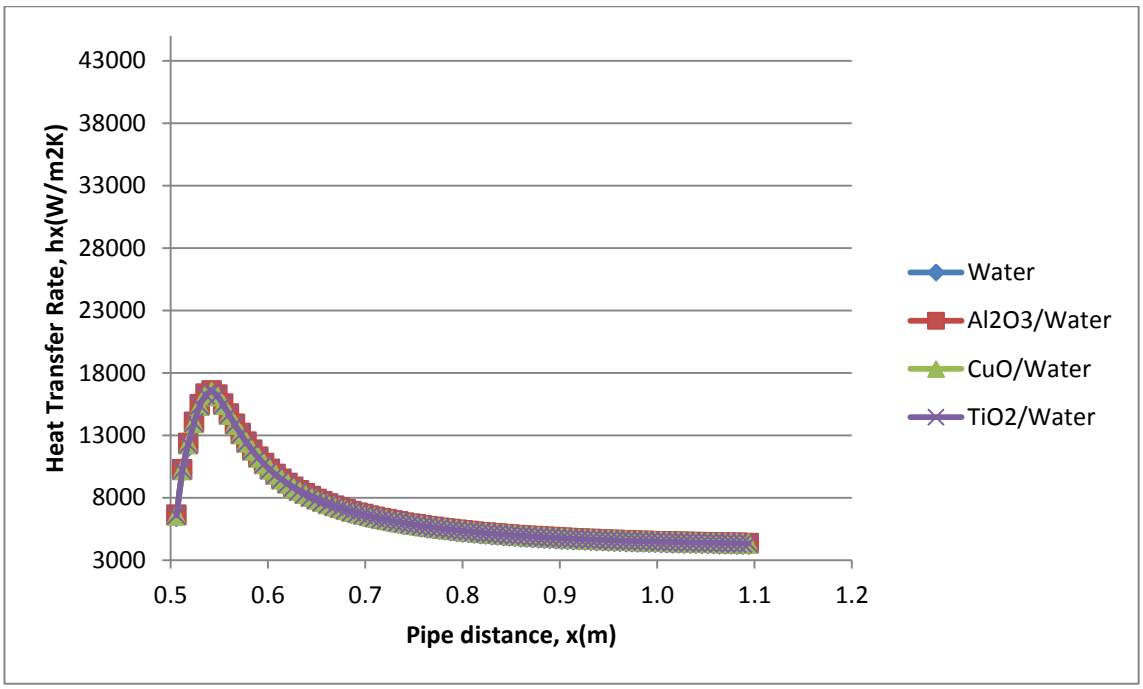

Figure 4.11: The variation of heat transfer rate of nanofluids at Re=17050

Figure 4.12 shows the decreasing of heat transfer coefficient for all the nanofluids after the reattachment point. The highest value occur for Al_2O_3 at h = 29306 W/m^{2}K. The average value of heat transfer coefficient for Al_2O_3 is 3% higher than water.

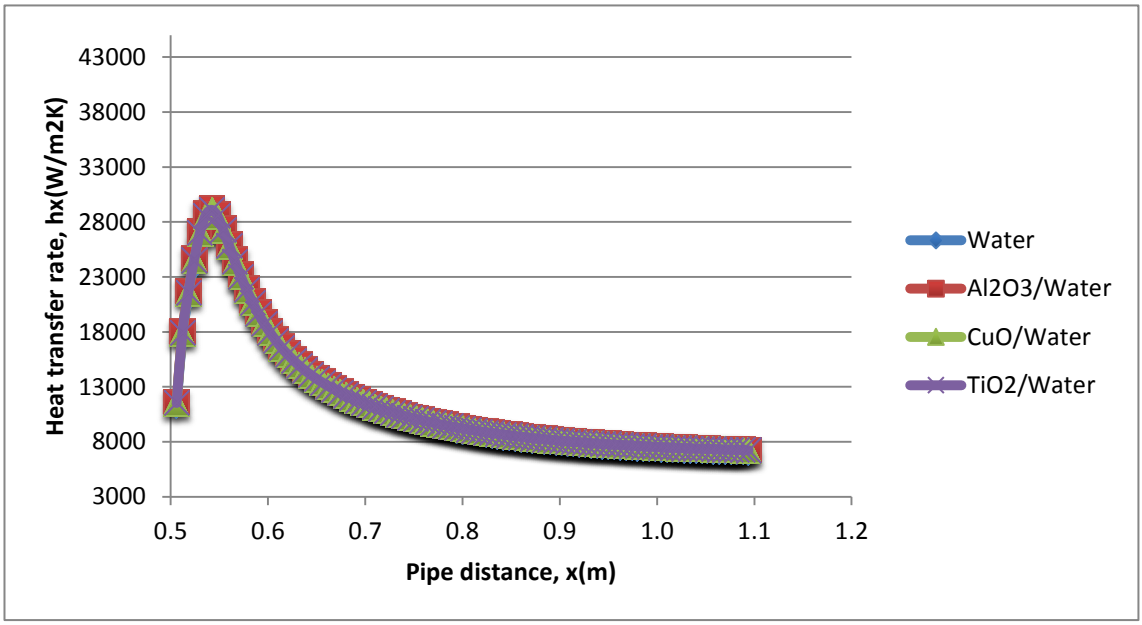

Figure 4.12: The variation of heat transfer rate of nanofluids at Re=30720

It was observed that when the value of Reynolds number keep increase at 44545, there is no different between the heat transfer rate for all the nanofluids with the water, as shown in Figure 4.13. Increasing of flow Reynolds number, results in increasing of turbulent eddies. High heat transfer is obtained and decreased sharply after reattachment point. Reynolds number of 44545 shows the highest heat transfer rate which decreases proportionally with increase of Reynolds number.

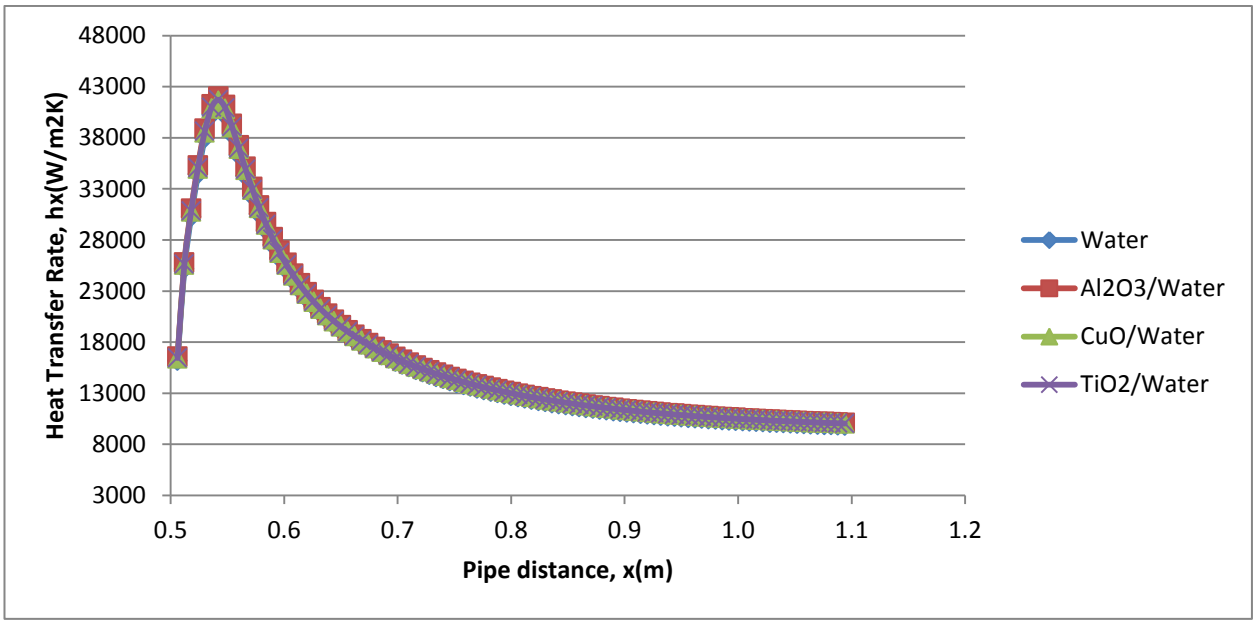

Figure 4.13: The variation of heat transfer rate of nanofluids at Re=44545

Figure 4.14 shows the relationship between temperature distribution and heat transfer rate for Al_2O_3/water for various Reynolds number. This event causes increasing of effective thermal conductivity of nanofluid and consequently increasing of convective heat transfer.

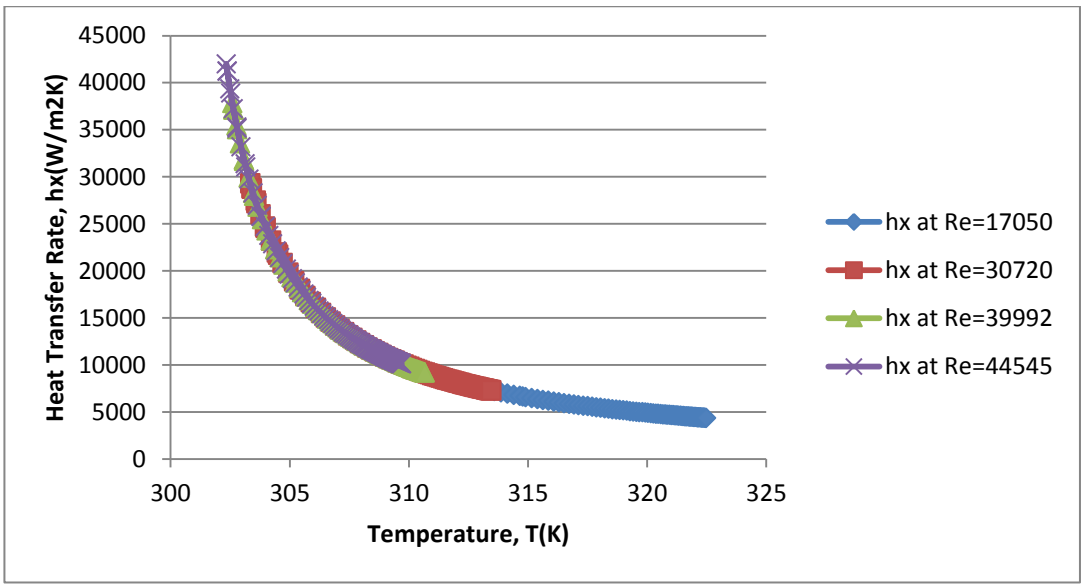

Figure 4.14: The variation of heat transfer rate with surface temperature for Al_2O_3/Water

The graph in Figure 4.15 shows result for nanofluids with 2% volume fraction at step height 13.5mm. From the observation, the low value of Reynolds number caused the fluid to have low value of heat transfer coefficient. It is prove that the Reynolds number and heat transfer coefficient proportional to each other at constant volume fraction and heat flux. The Al_2O_3/water shows the highest distribution of heat transfer rate for each Reynolds number, which 3% higher than water.

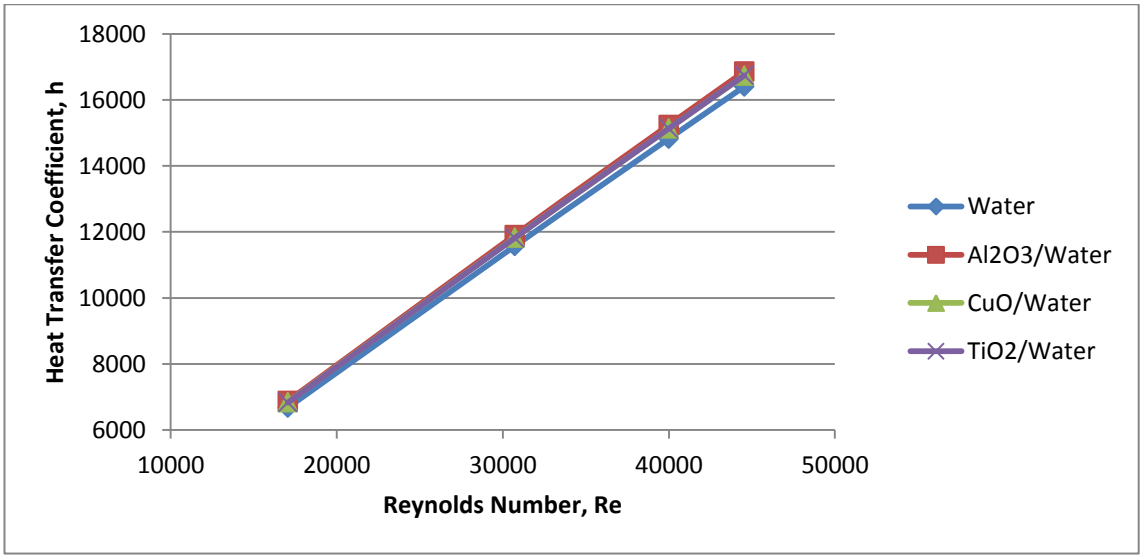

Figure 4.15 : Heat transfer coefficient versus Reynolds Number (at step height 13.5mm and volume fraction 2%)

4.5 Nusselt number

Figure 4.16, Figure 4.17, Figure 4.18 and Figure 4.19, shows a variations of Nusselt number versus pipe distance for water and nanofluids at various Reynolds number. The value of Nusselt number depends on heat transfer coefficient, distance and thermal conductivity of the fluid flow. Generally, the Nusselt number start to increase when entering the heated pipe due to high heat transfer coefficient at the area. After the reattachment point, due to the backward facing step effect, the value start to decrease sharply for all the nanofluids. Reynolds number of 17050 presented the lowest Nusselt number for all the working fluids and the highest Nusselt number obtained from Re=44545. The increase of Reynolds number will also increase the value of Nusselt number, thus explaining the condition of heat transfer rate for the system. The highest Nusselt number is approximately 2000 for the heat flux 49050 W/m^2. The value can be observed at the position of reattachment point for all the cases where the heat transfer coefficient at maximum value. There are similar curve pattern for the nanofluids and water.

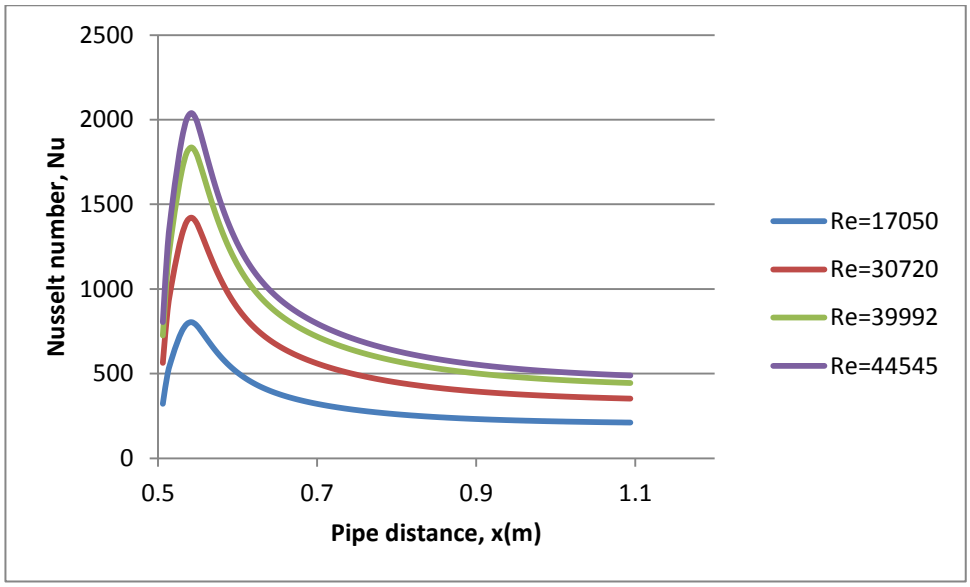

Figure 4.16: The Nusselt number variation of water with pipe distance

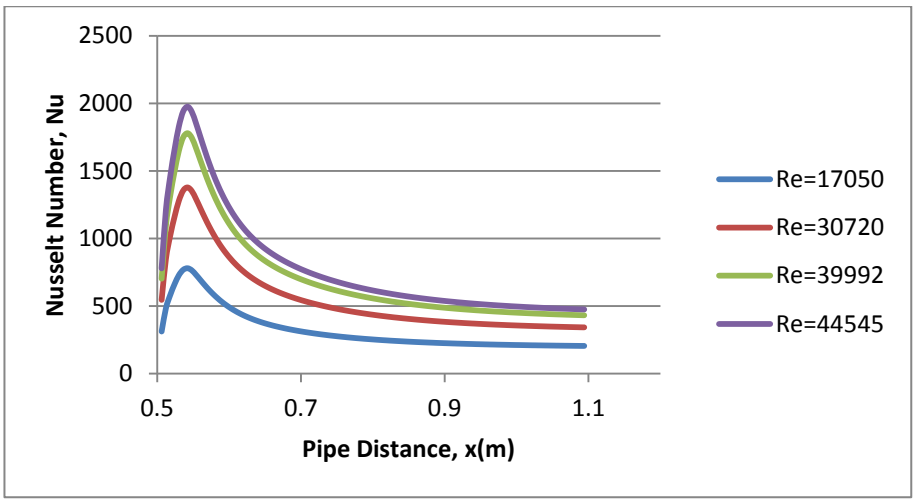

Figure 4.17: The Nusselt number variation of Al2O3/water with pipe distance

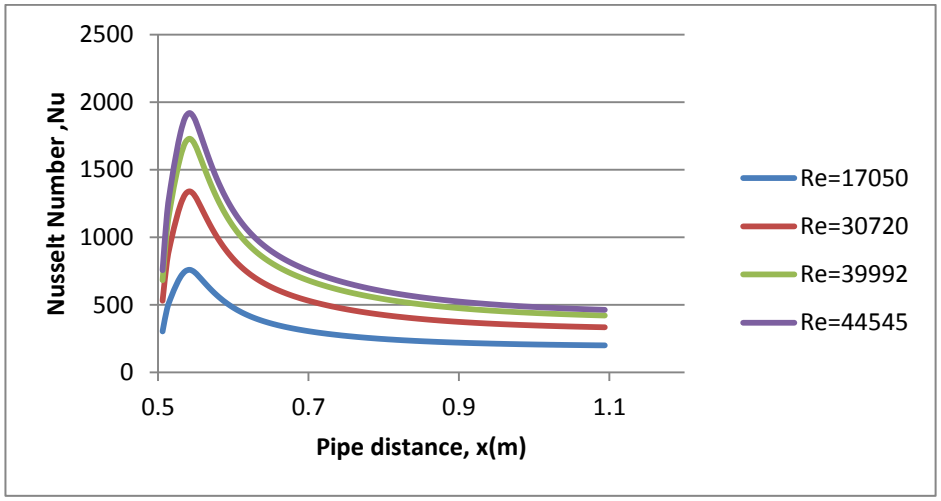

Figure 4.18: The Nusselt number variation of CuO/water with pipe distance

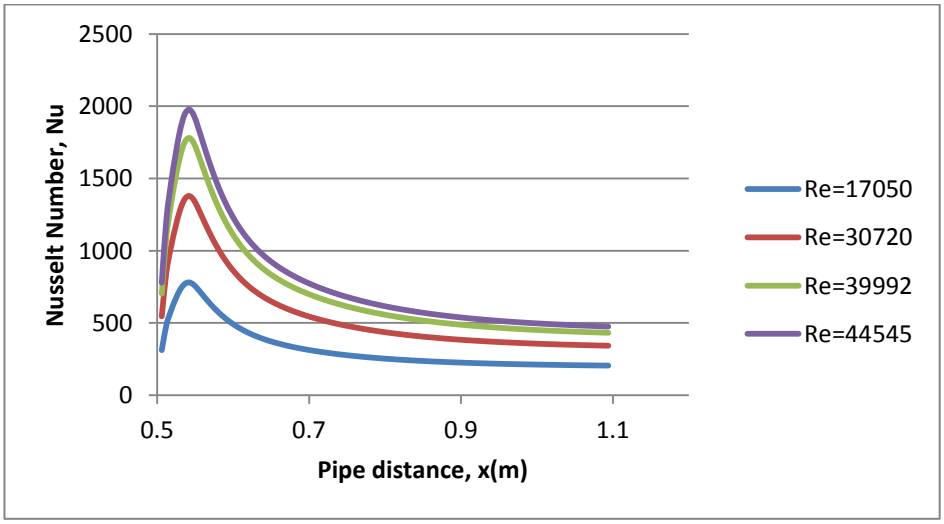

Figure 4.19: The Nusselt number variation of TiO_2/water with pipe distance

The comparison of Nusselt number between all the working fluids applied at the heated section shown in Figure 4.20. Reynolds number with the highest value seems to show the rapid increase of Nusselt number at the reattachment point and give a maximum value for all the nanofluids.

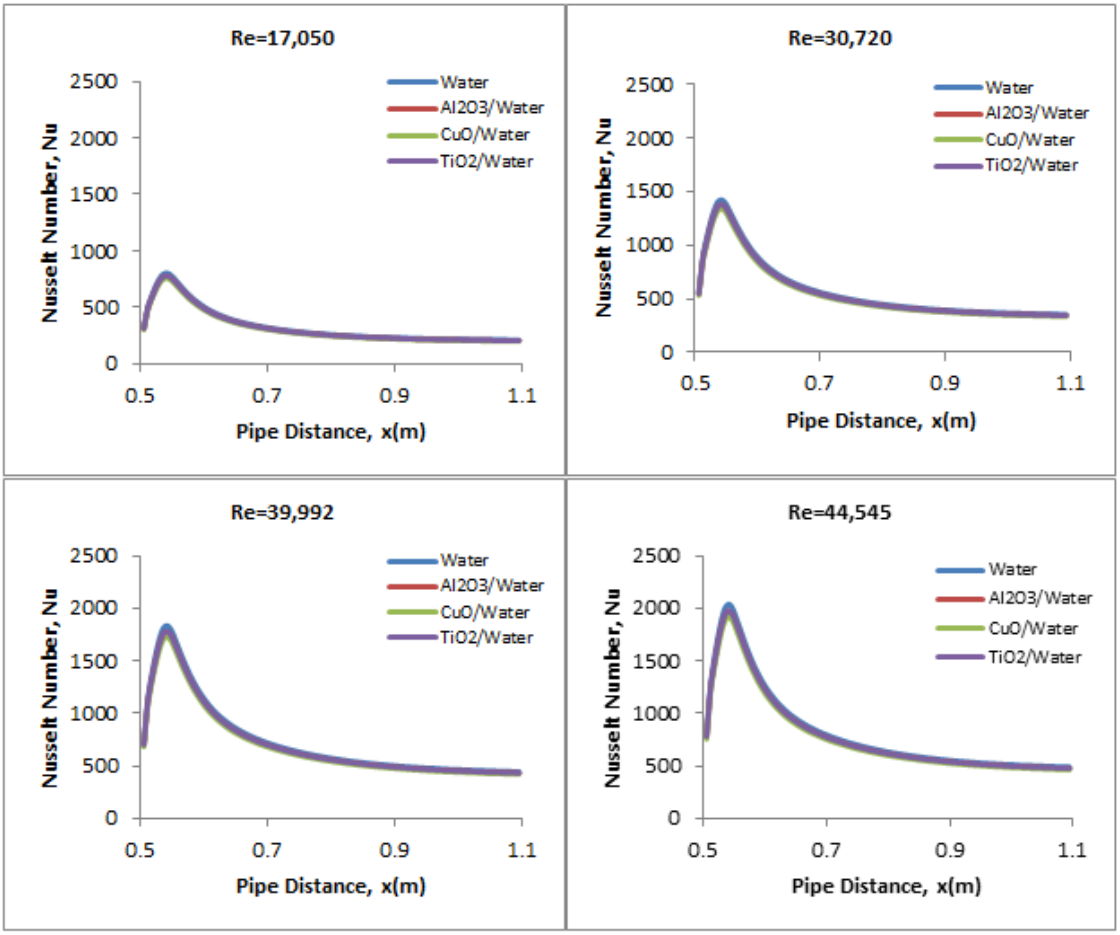

Figure 4.20: Comparison between the working fluids with various Reynolds Number

The pattern of flow overlapping each other with the water but less about 3% for Al_2O_3 and TiO_3 and 5% for CuO. The diagram shows that, at Reynolds number 17050, CuO will return high Nusselt number compared to other nanofluids which the lowest in the current testing.

4.6 Variation of Step Height

The graph in Figure 4.21 shows result for Nusselt number versus axial distance for CuO (2%)/water at different step height.The surface temperature distribution decreases as the step height increases especially in the separation region, directly behind the step for the same Reynolds number and surface heat flux. The separation region behind the step increases as the step height increases. Separation creates a recirculated flow moving towards the step at the heated tube surface which then drifts away from the step by the main separated flow. High value of step height produced high Nusselt number for each type of Reynolds number. The amount of Nusselt number rapidly increase after the step and decrease slowly after the reattachment point. The maximum value of Nusselt number occur at Re=44545 for step height 18.5mm. Value of Nusselt number at step height 6mm nearly constant along the heated pipe with constant heat flux.

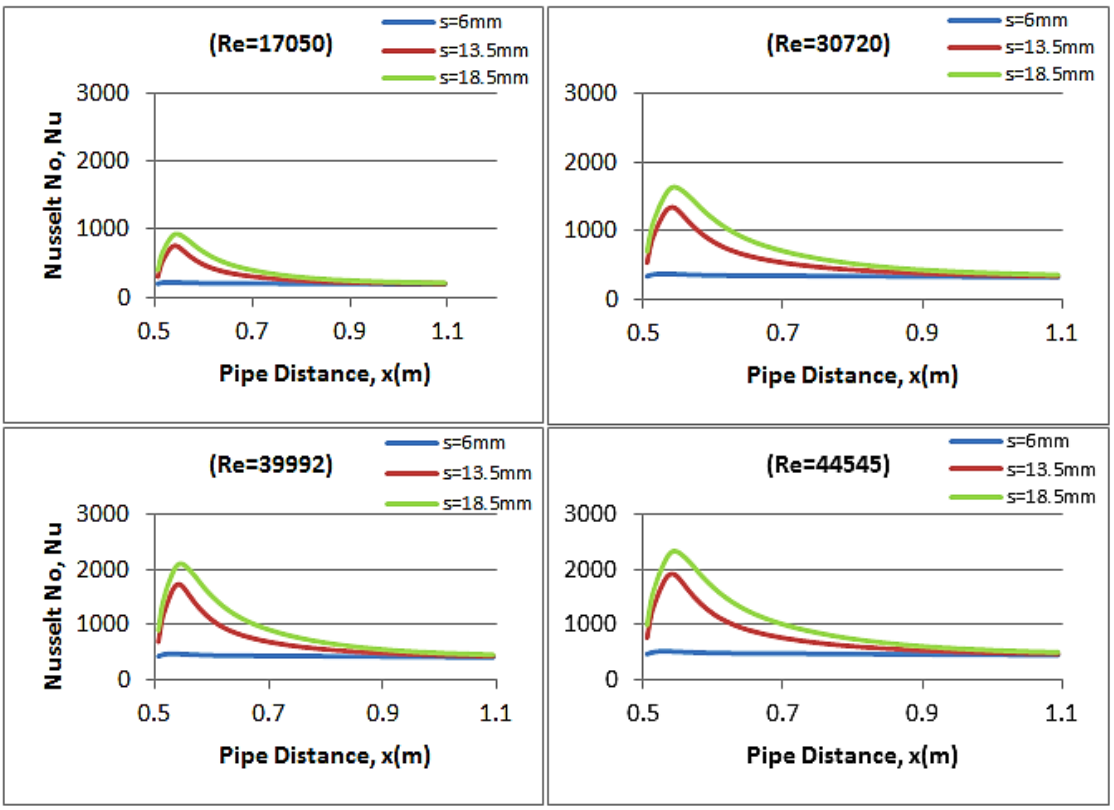

Figure 4.21: Variation of step heights for CuO/water at 2% volume fraction

4.7 Variation of Particle Concentrations

The graph in Figure 4.22 shows variations of local heat transfer coefficient with axial distance for three particles concentration of Al_2O_3/water.The value (h_x) increases until it reaches a maximum at the reattachment point (maximum heat transfer point) after which (h_x) decreases asymptotically while moving along the X-axis towards the test section exit. For the same heat flux and Re number, the h_x increases as the volume fraction increases, especially in the separation region due to more induced vortex. In the separation region, the improvement of (h_x) is quite clear in comparison to the local heat transfer coefficient (h_x) obtained for the flow with higher Reynolds number(Re=44545) and high particle concentration(2%). The volume fraction of 0.5% and 1.0% caused the flow to have nearly constant of heat transfer coefficient value, with slight increased at the reattachment point.

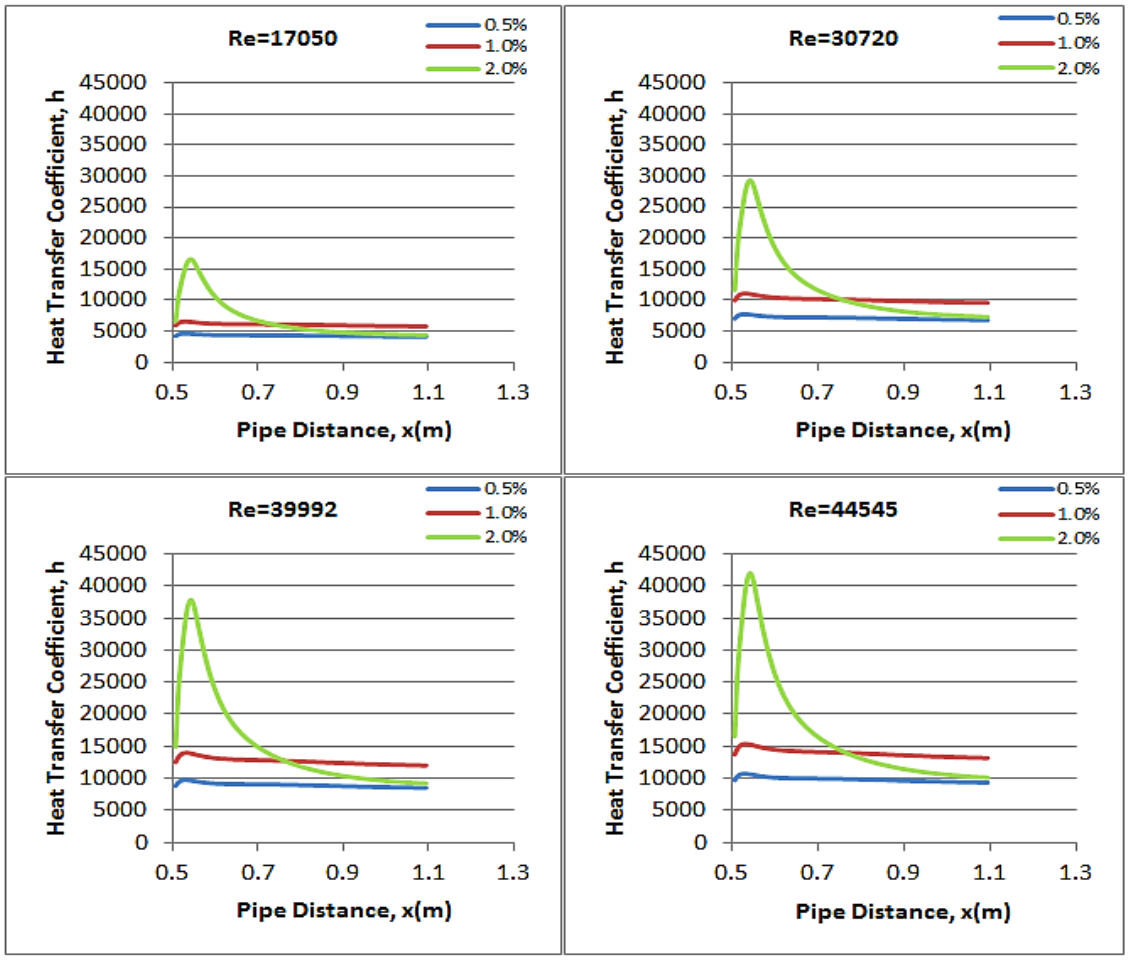

Figure 4.22: Variation of volume fraction for Al_2O_3/water at 13.5mm step height

CHAPTER 5: CONCLUSION AND RECOMMENDATION

5.1 Conclusion

The primary aim of this study is to identify the performance of three type of nanoluids : Al_2O_3, at 0.5%, 1% and 2% concentration and CuO and TiO_2 with 2% concentration over the base fluid water. The model considered is an heat exchanger tube with sudden expansion, having a various step height, S=6.0mm, 13.5mm and 18.5mm for CuO/water and constant step height for Al_2O_3 and TiO_2, heated with uniform heat flux, q=49050 W/m^2. This geometries is evaluated and simulate using CFD software package ANSYS 14.0. The solver used standard k-ε turbulence model in calculating the solution for the flow field given by Reynolds number 17050, 302720, 39992 and 44545 for both uniform flow and fully developed turbulent flow.

From the simulation, the flow separation is confirmed to have a reduction of temperature at the reattachment point just after the step for the same model having constant step height and heat flux. The investigation shows that the increase of Reynolds number will reduce the surface temperature at the reattachment zone. The lowest temperature will occur at this area and shows the location of reattachment point. The surface temperature will increase gradually with the pipe distance for all the nanofluids applied.

At the reattachment point of backward facing step, the heat transfer coefficient and Nusselt number appeared to be maximum with the minimum of surface temperature. The value start to decrease rapidly after the separation zone and it appears similar for all the cases. The increase of Reynolds number, will increase the value of Nusselt number and heat transfer coefficient. The value of Nusselt number also has a close effect with the length and thermal conductivity of the nanofluids.

5.2 Recommendation

This computational analysis can be extended to consider other parameter as well. The volume fraction variations of nanoparticles will lead to a better understanding of particle concentration and heat transfer rate relationship. More precise result can be observed with the increase of mesh interval, up to 0.1 size. The step height of sudden expansion give a different effect on backward facing step, and this could be a recommended for future study. The model of nanofluids analyze in this study shows a good agreement with the basic water flow and can be used as guidance for further analysis on fluid flow for other thermophysical properties of nanofluids.

REFERENCES

Abu-Nada, E., 2008. Application of nanofluids for heat transfer enhancement of separated flows encountered in a backward facing step. , 29, pp.242–249.

Al-aswadi, a. a. A. et al., 2010. Laminar forced convection flow over a backward facing step using nanofluids. *International Communications in Heat and Mass Transfer*, 37(8), pp.950–957.

Aminfar, H., Motallebzadeh, R. & Farzadi, A., 2010. The Study of the Effects of Thermophoretic and Brownian Forces on Nanofluid Thermal Conductivity Using Lagrangian and Eulerian Approach. *Nanoscale and Microscale Thermophysical Engineering*, 14(4), pp.187–208.

Anderson, R., 2001. Exploring the mathematical and interpretative strategies of Maxwell's Treatise on Electricity and Magnetism. *Endeavour*, 25(4), pp.157–165.

Armalyt, B.B.F., Dursts, F. & Pereira, J.C.F., 1983. Experimental and theoretical investigation of backward-facing step flow. , 127.

Asirvatham, L.G. et al., 2009. Experimental Study on Forced Convective Heat Transfer with Low Volume Fraction of CuO/Water Nanofluid. *Energies*, 2(1), pp.97–110.

Bayat, J. & Nikseresht, A.H., 2012. Thermal performance and pressure drop analysis of nanofluids in turbulent forced convective flows. *International Journal of Thermal Sciences*, 60, pp.236–243.

Bhandari, D., 2012. ANALYSIS OF FULLY DEVELOPED TURBULENT FLOW IN A PIPE. , 1(5), pp.1–9.

Bianco, V., Manca, O. & Nardini, S., 2011. Numerical investigation on nanofluids turbulent convection heat transfer inside a circular tube. *International Journal of Thermal Sciences*, 50(3), pp.341–349.

Biswas, G., Breuer, M. & Durst, F., 2004. Backward-Facing Step Flows for Various Expansion Ratios at Low and Moderate Reynolds Numbers. *Journal of Fluids Engineering*, 126(3), p.362.

Fotukian, S.M. & Nasr Esfahany, M., 2010. Experimental investigation of turbulent convective heat transfer of dilute γ-Al2O3/water nanofluid inside a circular tube. *International Journal of Heat and Fluid Flow*, 31(4), pp.606–612.

Furuichi, N., Hachiga, T. & Kumada, M., 2004. An experimental investigation of a large-scale structure of a two-dimensional backward-facing step by using advanced multi-point LDV. *Experiments in Fluids*, 36(2), pp.274–281.

Gavtash, B. et al., 2012. Numerical Simulation of the Effects of Nanofluid on a Heat Pipe Thermal Performance. , pp.549–555.

Ghadimi, A., Saidur, R. & Metselaar, H.S.C., 2011. A review of nanofluid stability properties and characterization in stationary conditions. *International Journal of Heat and Mass Transfer*, 54, pp.4051–4068.

Jonathan, Z., 2009. *Modeling Fluid Flow Using Fluent*,

Keshavarz Moraveji, M. & Razvarz, S., 2012. Experimental investigation of aluminum oxide nanofluid on heat pipe thermal performance. *International Communications in Heat and Mass Transfer*, 39(9), pp.1444–1448.

Ko, G.H. et al., 2007. An experimental study on the pressure drop of nanofluids containing carbon nanotubes in a horizontal tube. *International Journal of Heat and Mass Transfer*, 50(23-24), pp.4749–4753.

Kumar, A. & Dhiman, A.K., 2012. Effect of a circular cylinder on separated forced convection at a backward-facing step. *International Journal of Thermal Sciences*, 52, pp.176–185.

Lan, H., Armaly, B.F. & Drallmeier, J. a., 2009. Three-dimensional simulation of turbulent forced convection in a duct with backward-facing step. *International Journal of Heat and Mass Transfer*, 52(7-8), pp.1690–1700.

Lancial, N. et al., 2013. Effects of a turbulent wall jet on heat transfer over a non-confined backward-facing step. *International Journal of Heat and Fluid Flow*, 44, pp.336–347.

Liu, M., Lin, M.C. & Wang, C., 2011. Enhancements of thermal conductivities with Cu, CuO, and carbon nanotube nanofluids and application of MWNT/water nanofluid on a water chiller system. *Nanoscale research letters*, 6(1), p.297.

Maïga, S.E.B. et al., 2006. Heat transfer enhancement in turbulent tube flow using Al2O3 nanoparticle suspension. *International Journal of Numerical Methods for Heat & Fluid Flow*, 16(3), pp.275–292.

Mohammed, H. a. et al., 2011. Convective heat transfer and fluid flow study over a step using nanofluids: A review. *Renewable and Sustainable Energy Reviews*, 15(6), pp.2921–2939.

Nait Bouda, N. et al., 2008. Experimental approach and numerical prediction of a turbulent wall jet over a backward facing step. *International Journal of Heat and Fluid Flow*, 29(4), pp.927–944.

Oon, C.S. et al., 2013. Computational simulation of heat transfer to separation fluid flow in an annular passage. *International Communications in Heat and Mass Transfer*, 46, pp.92–96.

Prasad V.Tota, 2009. Turbulent Flow Over a Backward-Facing Step Using the RNG k-ε Model. *Flow Science*, (April), pp.1–15.

Rashmi, W. et al., 2013. Experimental and numerical investigation of heat transfer in CNT nanofluids. *Journal of Experimental Nanoscience*, 0(0), pp.1–19.

Roberts, N. a. & Walker, D.G., 2010. Convective Performance of Nanofluids in Commercial Electronics Cooling Systems. *Applied Thermal Engineering*, 30(16), pp.2499–2504.

Rostamani, M. et al., 2010. Numerical study of turbulent forced convection flow of nanofluids in a long horizontal duct considering variable properties. *International Communications in Heat and Mass Transfer*, 37(10), pp.1426–1431.

Roy, G. et al., 2012. Heat transfer performance and hydrodynamic behavior of turbulent nanofluid radial flows. *International Journal of Thermal Sciences*, 58, pp.120–129.

Saeedinia, M., Akhavan-Behabadi, M. a. & Nasr, M., 2012. Experimental study on heat transfer and pressure drop of nanofluid flow in a horizontal coiled wire inserted tube under constant heat flux. *Experimental Thermal and Fluid Science*, 36, pp.158–168.

Saffari Pour, M., 2012. Numerical Investigation Of Forced Laminar Convection Flow Of Nanofluids Over A Backward Facing Step Under Bleeding Condition. *Journal of Mechanics*, 28(June), pp.559–564.

Saidur, R., Leong, K.Y. & Mohammad, H.A., 2011. A review on applications and challenges of nanofluids. *Renewable and Sustainable Energy Reviews*, 15(3), pp.1646–1668.

Sajadi, a. R. & Kazemi, M.H., 2011. Investigation of turbulent convective heat transfer and pressure drop of TiO2/water nanofluid in circular tube. *International Communications in Heat and Mass Transfer*, 38(10), pp.1474–1478.

Saldana, J.G.B., Anand, N.K. & Sarin, V., 2005a. Numerical Simulation of Mixed Convective Flow Over a Three-Dimensional Horizontal Backward Facing Step. *Journal of Heat Transfer*, 127(9), p.1027.

Saldana, J.G.B., Anand, N.K. & Sarin, V., 2005b. Numerical Simulation of Mixed Convective Flow Over a Three-Dimensional Horizontal Backward Facing Step. *Journal of Heat Transfer*, 127(9), p.1027.

Singh, A.P., Paul, A.R. & Ranjan, P., 2011. Investigation of reattachment length for a turbulent flow over a backward facing step for different step angle. , 3(2), pp.84–88.

Sonawane, S. et al., 2011. An experimental investigation of thermo-physical properties and heat transfer performance of Al2O3-Aviation Turbine Fuel nanofluids. *Applied Thermal Engineering*, 31(14-15), pp.2841–2849.

Stolpa, S., 2004. Turbulent Heat Transfer.

Sundar, L.S. & Sharma, K.V., 2010. Turbulent heat transfer and friction factor of Al2O3 Nanofluid in circular tube with twisted tape inserts. *International Journal of Heat and Mass Transfer*, 53(19-20), pp.1409–1416.

Sureshkumar, R., Mohideen, S.T. & Nethaji, N., 2013. Heat transfer characteristics of nanofluids in heat pipes: A review. *Renewable and Sustainable Energy Reviews*, 20, pp.397–410.

Taylor, P., Experimental Heat Transfer : A Journal of Thermal Energy Generation , Transport , Storage , and Conversion Hydrodynamic And Heat Transfer Study Of Dispersed Fluids With Submicron Metallic Oxide. , (November 2012), pp.37–41.

Teng, T.-P. et al., 2010. Thermal efficiency of heat pipe with alumina nanofluid. *Journal of Alloys and Compounds*, 504, pp.S380–S384.

Tihon, J. et al., 2012. The transitional backward-facing step flow in a water channel with variable expansion geometry. *Experimental Thermal and Fluid Science*, 40, pp.112–125.

Togun, H. et al., 2011. An experimental study of heat transfer to turbulent separation fluid flow in an annular passage. *International Journal of Heat and Mass Transfer*, 54(4), pp.766–773.

Wang, W., Zhang, L. & Yan, Y., 2012. Large eddy simulation of turbulent flow downstream of a backward-facing step. *Procedia Engineering*, 31, pp.16–22.

Wang, X. & Mujumdar, A.S., 2006. Heat transfer characteristics of nanofluids : a review. *International Journal of Thermal Sciences*, 46, pp.1–19.

Wang, X.-Q. & Mujumdar, A.S., 2007. Heat transfer characteristics of nanofluids: a review. *International Journal of Thermal Sciences*, 46(1), pp.1–19.

Xuan, Y. & Roetzel, W., 2000. Conceptions for heat transfer correlation of nano ¯ uids. , 43, pp.3701–3707.

Yang, J.-C. et al., 2013. Experimental study on the characteristics of heat transfer and flow resistance in turbulent pipe flows of viscoelastic-fluid-based Cu nanofluid. *International Journal of Heat and Mass Transfer*, 62, pp.303–313.

Zeinali Heris, S., Nasr Esfahany, M. & Etemad, S.G., 2007. Experimental investigation of convective heat transfer of Al2O3/water nanofluid in circular tube. *International Journal of Heat and Fluid Flow*, 28(2), pp.203–210.

APPENDICES

NUMERICAL SIMULATION DATA FOR TEMPERATURE DISTRIBUTION

Table 6.1 : Surface temperature data using nanofluids Water

Re	17050	30720	39992	44545
X [m]	Temperature [K]	Temperature [K]	Temperature [K]	Temperature [K]
0.50600	315.17868	308.66605	306.73090	306.06888
0.51200	309.78986	305.57642	304.32672	303.89948
0.51800	308.13971	304.63348	303.59430	303.23914
0.52400	307.15027	304.07373	303.16144	302.84961
0.53000	306.50433	303.69940	302.86926	302.58569
0.53600	306.16412	303.49280	302.70526	302.43665
0.54200	306.07196	303.43436	302.65845	302.39392
0.54800	306.19757	303.50244	302.71072	302.44092
0.55400	306.48569	303.66675	302.83893	302.55682
0.56000	306.84216	303.87268	303.00012	302.70276
0.56600	307.23682	304.10089	303.17883	302.86444
0.57200	307.65320	304.34204	303.36762	303.03534
0.57800	308.08005	304.58923	303.56116	303.21045
0.58400	308.51135	304.83884	303.75653	303.38718
0.59000	308.94275	305.08859	303.95190	303.56393
0.59600	309.37048	305.33630	304.14575	303.73926
0.60200	309.79144	305.58011	304.33649	303.91180
0.60800	310.20331	305.81873	304.52319	304.08063
0.61400	310.60461	306.05127	304.70508	304.24515
0.62000	310.99445	306.27719	304.88184	304.40497
0.62600	311.37238	306.49628	305.05319	304.55994
0.63200	311.73834	306.70844	305.21912	304.70999
0.63800	312.09253	306.91376	305.37970	304.85516
0.64400	312.43530	307.11252	305.53513	304.99570
0.65000	312.76727	307.30505	305.68567	305.13181
0.65600	313.08899	307.49176	305.83167	305.26379
0.66200	313.40106	307.67304	305.97348	305.39203
0.66800	313.70422	307.84930	306.11145	305.51679
0.67400	313.99902	308.02100	306.24588	305.63843
0.68000	314.28595	308.18842	306.37708	305.75714
0.68600	314.56549	308.35187	306.50531	305.87323
0.69200	314.83804	308.51160	306.63074	305.98682
0.69800	315.10394	308.66791	306.75360	306.09818
0.70400	315.36353	308.82089	306.87402	306.20734
0.71000	315.61707	308.97073	306.99213	306.31448

0.71600	315.86481	309.11762	307.10803	306.41968
0.72200	316.10696	309.26166	307.22186	306.52301
0.72800	316.34360	309.40292	307.33362	306.62451
0.73400	316.57483	309.54150	307.44336	306.72424
0.74000	316.80072	309.67737	307.55115	306.82221
0.74600	317.02142	309.81061	307.65692	306.91840
0.75200	317.23688	309.94125	307.76080	307.01294
0.75800	317.44721	310.06928	307.86273	307.10574
0.76400	317.65247	310.19473	307.96277	307.19690
0.77000	317.85263	310.31760	308.06088	307.28635
0.77600	318.04776	310.43790	308.15710	307.37415
0.78200	318.23785	310.55563	308.25140	307.46024
0.78800	318.42297	310.67084	308.34381	307.54468
0.79400	318.60315	310.78345	308.43433	307.62738
0.80000	318.77844	310.89356	308.52295	307.70844
0.80600	318.94894	311.00107	308.60971	307.78784
0.81200	319.11475	311.10608	308.69458	307.86551
0.81800	319.27600	311.20853	308.77753	307.94150
0.82400	319.43289	311.30850	308.85858	308.01581
0.83000	319.58554	311.40601	308.93774	308.08844
0.83600	319.73395	311.50110	309.01505	308.15942
0.84200	319.87811	311.59387	309.09055	308.22876
0.84800	320.01807	311.68439	309.16425	308.29651
0.85400	320.15387	311.77271	309.23627	308.36264
0.86000	320.28555	311.85883	309.30658	308.42725
0.86600	320.41321	311.94275	309.37524	308.49042
0.87200	320.53693	312.02454	309.44226	308.55212
0.87800	320.65677	312.10419	309.50769	308.61234
0.88400	320.77289	312.18170	309.57147	308.67114
0.89000	320.88538	312.25714	309.63364	308.72846
0.89600	320.99432	312.33048	309.69421	308.78436
0.90200	321.09982	312.40179	309.75324	308.83887
0.90800	321.20194	312.47110	309.81073	308.89200
0.91400	321.30078	312.53842	309.86670	308.94373
0.92000	321.39648	312.60382	309.92114	308.99414
0.92600	321.48908	312.66730	309.97412	309.04321
0.93200	321.57871	312.72894	310.02570	309.09100
0.93800	321.66544	312.78882	310.07581	309.13751
0.94400	321.74939	312.84692	310.12451	309.18274
0.95000	321.83060	312.90335	310.17188	309.22675
0.95600	321.90918	312.95813	310.21790	309.26953
0.96200	321.98523	313.01135	310.26267	309.31113
0.96800	322.05884	313.06296	310.30615	309.35159

0.97400	322.13007	313.11307	310.34845	309.39093
0.98000	322.19894	313.16171	310.38953	309.42920
0.98600	322.26559	313.20892	310.42947	309.46643
0.99200	322.33008	313.25476	310.46829	309.50263
0.99800	322.39249	313.29926	310.50604	309.53778
1.00400	322.45285	313.34244	310.54269	309.57199
1.01000	322.51123	313.38434	310.57831	309.60529
1.01600	322.56772	313.42505	310.61298	309.63763
1.02200	322.62235	313.46454	310.64661	309.66907
1.02800	322.67517	313.50287	310.67932	309.69965
1.03400	322.72626	313.54004	310.71112	309.72937
1.04000	322.77564	313.57617	310.74204	309.75830
1.04600	322.82343	313.61121	310.77203	309.78644
1.05200	322.86975	313.64520	310.80121	309.81378
1.05800	322.91473	313.67819	310.82959	309.84033
1.06400	322.95844	313.71021	310.85712	309.86615
1.07000	323.00089	313.74121	310.88388	309.89130
1.07600	323.04208	313.77130	310.90985	309.91568
1.08200	323.08212	313.80042	310.93506	309.93936
1.08800	323.12054	313.82858	310.95950	309.96234
1.09400	323.16028	313.85657	310.98361	309.98496

Table 6.2 : Surface temperature data using nanofluids Al_2O_3/Water

Re	17050	30720	39992	44545
X [m]	Temperature [K]	Temperature [K]	Temperature [K]	Temperature [K]
0.50600	314.78320	308.44989	306.56628	305.92145
0.51200	309.52728	305.43323	304.21777	303.80200
0.51800	307.92255	304.51508	303.50427	303.15860
0.52400	306.96112	303.97049	303.08289	302.77930
0.53000	306.33325	303.60620	302.79837	302.52228
0.53600	306.00189	303.40485	302.63849	302.37689
0.54200	305.91126	303.34735	302.59241	302.33490
0.54800	306.03186	303.41281	302.64273	302.38013
0.55400	306.31030	303.57181	302.76685	302.49240
0.56000	306.65527	303.77130	302.92316	302.63391
0.56600	307.03742	303.99262	303.09650	302.79083
0.57200	307.44070	304.22644	303.27972	302.95667
0.57800	307.85413	304.46619	303.46756	303.12665
0.58400	308.27188	304.70828	303.65714	303.29819
0.59000	308.68976	304.95053	303.84680	303.46976
0.59600	309.10407	305.19077	304.03491	303.63995
0.60200	309.51178	305.42722	304.22003	303.80743
0.60800	309.91071	305.65863	304.40118	303.97131
0.61400	310.29935	305.88416	304.57770	304.13098
0.62000	310.67688	306.10327	304.74921	304.28613
0.62600	311.04291	306.31570	304.91550	304.43652
0.63200	311.39734	306.52145	305.07651	304.58215
0.63800	311.74036	306.72058	305.23233	304.72305
0.64400	312.07233	306.91333	305.38312	304.85944
0.65000	312.39380	307.10004	305.52921	304.99152
0.65600	312.70532	307.28107	305.67087	305.11963
0.66200	313.00757	307.45685	305.80847	305.24405
0.66800	313.30115	307.62778	305.94232	305.36514
0.67400	313.58661	307.79425	306.07275	305.48315
0.68000	313.86447	307.95654	306.20007	305.59839
0.68600	314.13519	308.11505	306.32446	305.71103
0.69200	314.39911	308.26996	306.44617	305.82129
0.69800	314.65659	308.42151	306.56537	305.92932
0.70400	314.90796	308.56982	306.68219	306.03528
0.71000	315.15347	308.71509	306.79675	306.13922
0.71600	315.39340	308.85754	306.90918	306.24127
0.72200	315.62787	308.99719	307.01959	306.34155
0.72800	315.85703	309.13416	307.12802	306.44006

0.73400	316.08093	309.26849	307.23450	306.53680
0.74000	316.29974	309.40027	307.33905	306.63184
0.74600	316.51343	309.52942	307.44171	306.72522
0.75200	316.72211	309.65607	307.54248	306.81693
0.75800	316.92584	309.78021	307.64136	306.90698
0.76400	317.12463	309.90186	307.73840	306.99542
0.77000	317.31848	310.02100	307.83362	307.08225
0.77600	317.50751	310.13763	307.92694	307.16742
0.78200	317.69165	310.25183	308.01843	307.25098
0.78800	317.87097	310.36353	308.10809	307.33289
0.79400	318.04550	310.47272	308.19592	307.41318
0.80000	318.21533	310.57947	308.28192	307.49182
0.80600	318.38052	310.68378	308.36609	307.56885
0.81200	318.54117	310.78558	308.44840	307.64426
0.81800	318.69742	310.88495	308.52887	307.71802
0.82400	318.84949	310.98193	308.60754	307.79013
0.83000	318.99741	311.07654	308.68439	307.86063
0.83600	319.14124	311.16876	308.75943	307.92950
0.84200	319.28101	311.25876	308.83270	307.99683
0.84800	319.41669	311.34656	308.90424	308.06256
0.85400	319.54834	311.43225	308.97412	308.12677
0.86000	319.67603	311.51581	309.04236	308.18951
0.86600	319.79981	311.59729	309.10904	308.25085
0.87200	319.91980	311.67664	309.17410	308.31073
0.87800	320.03607	311.75391	309.23761	308.36923
0.88400	320.14874	311.82916	309.29953	308.42633
0.89000	320.25787	311.90241	309.35992	308.48200
0.89600	320.36359	311.97363	309.41876	308.53632
0.90200	320.46597	312.04285	309.47607	308.58923
0.90800	320.56509	312.11017	309.53186	308.64087
0.91400	320.66107	312.17557	309.58624	308.69110
0.92000	320.75397	312.23908	309.63916	308.74008
0.92600	320.84393	312.30075	309.69064	308.78778
0.93200	320.93100	312.36066	309.74072	308.83417
0.93800	321.01526	312.41882	309.78943	308.87940
0.94400	321.09686	312.47534	309.83679	308.92334
0.95000	321.17578	312.53021	309.88281	308.96613
0.95600	321.25220	312.58350	309.92755	309.00772
0.96200	321.32617	312.63522	309.97107	309.04816
0.96800	321.39777	312.68543	310.01337	309.08752
0.97400	321.46704	312.73419	310.05450	309.12579
0.98000	321.53406	312.78156	310.09448	309.16299
0.98600	321.59897	312.82752	310.13330	309.19919

0.99200	321.66177	312.87213	310.17108	309.23438
0.99800	321.72253	312.91547	310.20779	309.26862
1.00400	321.78137	312.95755	310.24347	309.30194
1.01000	321.83829	312.99841	310.27820	309.33432
1.01600	321.89337	313.03806	310.31189	309.36581
1.02200	321.94663	313.07654	310.34467	309.39642
1.02800	321.99817	313.11395	310.37653	309.42621
1.03400	322.04800	313.15024	310.40753	309.45520
1.04000	322.09622	313.18549	310.43762	309.48337
1.04600	322.14291	313.21967	310.46689	309.51074
1.05200	322.18820	313.25287	310.49533	309.53742
1.05800	322.23218	313.28510	310.52295	309.56329
1.06400	322.27490	313.31638	310.54984	309.58850
1.07000	322.31644	313.34671	310.57593	309.61298
1.07600	322.35675	313.37610	310.60132	309.63678
1.08200	322.39594	313.40460	310.62592	309.65991
1.08800	322.43359	313.43213	310.64978	309.68231
1.09400	322.47253	313.45953	310.67328	309.70441

Table 6.3 : Surface temperature data using nanofluids CuO/Water

Re	17050	30720	39992	44545
X [m]	Temperature [K]	Temperature [K]	Temperature [K]	Temperature [K]
0.50600	308.52954	314.90753	306.63092	305.98108
0.51200	305.48090	309.60086	304.25659	303.83786
0.51800	304.55533	307.98483	303.53699	303.18878
0.52400	304.00665	307.01733	303.11224	302.80637
0.53000	303.63953	306.38532	302.82538	302.54718
0.53600	303.43634	306.05121	302.66400	302.40042
0.54200	303.37787	305.95892	302.61713	302.35770
0.54800	303.44312	306.07904	302.66730	302.40280
0.55400	303.60254	306.35782	302.79181	302.51544
0.56000	303.80280	306.70364	302.94879	302.65759
0.56600	304.02502	307.08698	303.12296	302.81525
0.57200	304.25992	307.49158	303.30710	302.98200
0.57800	304.50076	307.90637	303.49585	303.15289
0.58400	304.74399	308.32553	303.68640	303.32532
0.59000	304.98734	308.74481	303.87701	303.49783
0.59600	305.22870	309.16052	304.06607	303.66895
0.60200	305.46625	309.56958	304.25214	303.83731
0.60800	305.69870	309.96982	304.43420	304.00208
0.61400	305.92523	310.35977	304.61163	304.16260
0.62000	306.14536	310.73859	304.78400	304.31854
0.62600	306.35877	311.10580	304.95111	304.46973
0.63200	306.56543	311.46137	305.11292	304.61609
0.63800	306.76544	311.80548	305.26953	304.75775
0.64400	306.95905	312.13855	305.42108	304.89484
0.65000	307.14658	312.46100	305.56787	305.02759
0.65600	307.32840	312.77356	305.71021	305.15637
0.66200	307.50494	313.07678	305.84848	305.28143
0.66800	307.67664	313.37128	305.98297	305.40314
0.67400	307.84381	313.65762	306.11408	305.52179
0.68000	308.00684	313.93634	306.24197	305.63757
0.68600	308.16602	314.20789	306.36697	305.75079
0.69200	308.32163	314.47266	306.48926	305.86157
0.69800	308.47382	314.73096	306.60904	305.97015
0.70400	308.62280	314.98309	306.72644	306.07666
0.71000	308.76868	315.22943	306.84155	306.18115
0.71600	308.91174	315.47009	306.95453	306.28369
0.72200	309.05200	315.70532	307.06546	306.38446

0.72800	309.18955	315.93518	307.17438	306.48346
0.73400	309.32446	316.15982	307.28137	306.58072
0.74000	309.45679	316.37930	307.38641	306.67624
0.74600	309.58655	316.59369	307.48956	306.77008
0.75200	309.71375	316.80304	307.59082	306.86224
0.75800	309.83844	317.00742	307.69019	306.95276
0.76400	309.96060	317.20685	307.78766	307.04163
0.77000	310.08026	317.40140	307.88330	307.12888
0.77600	310.19742	317.59103	307.97711	307.21448
0.78200	310.31207	317.77582	308.06903	307.29846
0.78800	310.42429	317.95575	308.15915	307.38080
0.79400	310.53400	318.13089	308.24738	307.46149
0.80000	310.64124	318.30133	308.33380	307.54056
0.80600	310.74600	318.46713	308.41840	307.61798
0.81200	310.84827	318.62836	308.50110	307.69373
0.81800	310.94812	318.78519	308.58200	307.76788
0.82400	311.04553	318.93784	308.66104	307.84039
0.83000	311.14056	319.08637	308.73828	307.91126
0.83600	311.23328	319.23077	308.81372	307.98053
0.84200	311.32367	319.37109	308.88736	308.04816
0.84800	311.41193	319.50732	308.95929	308.11426
0.85400	311.49805	319.63953	309.02951	308.17883
0.86000	311.58203	319.76779	309.09815	308.24191
0.86600	311.66388	319.89215	309.16516	308.30359
0.87200	311.74365	320.01263	309.23059	308.36380
0.87800	311.82135	320.12946	309.29443	308.42261
0.88400	311.89697	320.24268	309.35669	308.48004
0.89000	311.97058	320.35236	309.41742	308.53604
0.89600	312.04218	320.45862	309.47656	308.59067
0.90200	312.11182	320.56152	309.53424	308.64392
0.90800	312.17950	320.66119	309.59039	308.69580
0.91400	312.24524	320.75769	309.64505	308.74640
0.92000	312.30914	320.85114	309.69830	308.79565
0.92600	312.37116	320.94159	309.75009	308.84363
0.93200	312.43143	321.02921	309.80048	308.89035
0.93800	312.48993	321.11401	309.84949	308.93585
0.94400	312.54678	321.19611	309.89716	308.98010
0.95000	312.60199	321.27557	309.94348	309.02313
0.95600	312.65558	321.35251	309.98853	309.06500
0.96200	312.70764	321.42700	310.03235	309.10574
0.96800	312.75818	321.49908	310.07492	309.14539
0.97400	312.80725	321.56888	310.11633	309.18390
0.98000	312.85492	321.63648	310.15662	309.22138

0.98600	312.90122	321.70187	310.19574	309.25787
0.99200	312.94617	321.76520	310.23377	309.29334
0.99800	312.98978	321.82648	310.27075	309.32782
1.00400	313.03214	321.88580	310.30673	309.36139
1.01000	313.07330	321.94324	310.34171	309.39404
1.01600	313.11325	321.99884	310.37570	309.42578
1.02200	313.15204	322.05264	310.40875	309.45667
1.02800	313.18970	322.10468	310.44089	309.48669
1.03400	313.22626	322.15503	310.47211	309.51593
1.04000	313.26178	322.20380	310.50250	309.54434
1.04600	313.29627	322.25098	310.53204	309.57196
1.05200	313.32977	322.29681	310.56073	309.59888
1.05800	313.36227	322.34131	310.58862	309.62500
1.06400	313.39383	322.38458	310.61578	309.65045
1.07000	313.42444	322.42661	310.64215	309.67517
1.07600	313.45413	322.46747	310.66773	309.69922
1.08200	313.48291	322.50717	310.69260	309.72257
1.08800	313.51068	322.54532	310.71671	309.74524
1.09400	313.53839	322.58484	310.74051	309.76755

Table 6.4 : Surface temperature data using nanofluids TiO_2/Water

Re	17050	30720	39992	44545
X [m]	Temperature [K]	Temperature [K]	Temperature [K]	Temperature [K]
0.50600	314.88840	308.50989	306.61264	305.96320
0.51200	309.59531	305.47199	304.24768	303.82886
0.51800	307.97907	304.54727	303.52908	303.18091
0.52400	307.01074	303.99875	303.10468	302.79889
0.53000	306.37836	303.63184	302.81815	302.54004
0.53600	306.04468	303.42908	302.65710	302.39368
0.54200	305.95337	303.37122	302.61078	302.35138
0.54800	306.07492	303.43716	302.66144	302.39694
0.55400	306.35541	303.59735	302.78647	302.51004
0.56000	306.70288	303.79831	302.94391	302.65259
0.56600	307.08783	304.02121	303.11853	302.81061
0.57200	307.49405	304.25678	303.30304	302.97766
0.57800	307.91049	304.49823	303.49225	303.14887
0.58400	308.33130	304.74213	303.68317	303.32166
0.59000	308.75220	304.98615	303.87421	303.49445
0.59600	309.16950	305.22812	304.06366	303.66586
0.60200	309.58020	305.46631	304.25012	303.83453
0.60800	309.98200	305.69940	304.43262	303.99960
0.61400	310.37354	305.92658	304.61041	304.16046
0.62000	310.75385	306.14728	304.78314	304.31671
0.62600	311.12250	306.36127	304.95062	304.46820
0.63200	311.47952	306.56851	305.11279	304.61487
0.63800	311.82504	306.76910	305.26975	304.75678
0.64400	312.15942	306.96326	305.42163	304.89414
0.65000	312.48325	307.15131	305.56879	305.02716
0.65600	312.79706	307.33368	305.71146	305.15619
0.66200	313.10150	307.51074	305.85004	305.28156
0.66800	313.39722	307.68292	305.98486	305.40350
0.67400	313.68475	307.85059	306.11627	305.52240
0.68000	313.96463	308.01410	306.24448	305.63843
0.68600	314.23731	308.17374	306.36978	305.75189
0.69200	314.50317	308.32977	306.49237	305.86292
0.69800	314.76254	308.48242	306.61243	305.97174
0.70400	315.01572	308.63184	306.73010	306.07843
0.71000	315.26306	308.77820	306.84552	306.18317
0.71600	315.50473	308.92163	306.95874	306.28595
0.72200	315.74091	309.06232	307.06995	306.38696

0.72800	315.97174	309.20026	307.17917	306.48615
0.73400	316.19727	309.33557	307.28641	306.58362
0.74000	316.41766	309.46832	307.39172	306.67932
0.74600	316.63294	309.59845	307.49512	306.77338
0.75200	316.84314	309.72601	307.59662	306.86578
0.75800	317.04831	309.85107	307.69623	306.95648
0.76400	317.24854	309.97360	307.79395	307.04556
0.77000	317.44385	310.09363	307.88983	307.13300
0.77600	317.63422	310.21112	307.98383	307.21878
0.78200	317.81970	310.32611	308.07599	307.30292
0.78800	318.00034	310.43863	308.16632	307.38544
0.79400	318.17615	310.54865	308.25476	307.46631
0.80000	318.34720	310.65619	308.34140	307.54553
0.80600	318.51361	310.76123	308.42615	307.62311
0.81200	318.67542	310.86377	308.50909	307.69904
0.81800	318.83283	310.96390	308.59015	307.77332
0.82400	318.98596	311.06158	308.66937	307.84598
0.83000	319.13501	311.15686	308.74677	307.91699
0.83600	319.27988	311.24976	308.82233	307.98639
0.84200	319.42065	311.34039	308.89615	308.05420
0.84800	319.55731	311.42883	308.96820	308.12039
0.85400	319.68994	311.51514	309.03857	308.18506
0.86000	319.81854	311.59934	309.10733	308.24829
0.86600	319.94321	311.68140	309.17447	308.31003
0.87200	320.06406	311.76135	309.24002	308.37036
0.87800	320.18115	311.83917	309.30399	308.42926
0.88400	320.29465	311.91498	309.36636	308.48676
0.89000	320.40460	311.98871	309.42719	308.54285
0.89600	320.51108	312.06043	309.48645	308.59753
0.90200	320.61420	312.13019	309.54416	308.65088
0.90800	320.71405	312.19797	309.60037	308.70282
0.91400	320.81070	312.26382	309.65512	308.75348
0.92000	320.90430	312.32776	309.70844	308.80280
0.92600	320.99487	312.38989	309.76028	308.85080
0.93200	321.08258	312.45023	309.81073	308.89755
0.93800	321.16745	312.50879	309.85980	308.94305
0.94400	321.24960	312.56567	309.90747	308.98737
0.95000	321.32910	312.62094	309.95383	309.03043
0.95600	321.40607	312.67456	309.99890	309.07233
0.96200	321.48059	312.72665	310.04273	309.11307
0.96800	321.55267	312.77722	310.08533	309.15271
0.97400	321.62244	312.82629	310.12674	309.19122
0.98000	321.69000	312.87396	310.16699	309.22870

0.98600	321.75534	312.92023	310.20612	309.26517
0.99200	321.81860	312.96512	310.24417	309.30063
0.99800	321.87982	313.00873	310.28113	309.33511
1.00400	321.93903	313.05109	310.31708	309.36865
1.01000	321.99634	313.09216	310.35202	309.40128
1.01600	322.05182	313.13208	310.38599	309.43298
1.02200	322.10547	313.17084	310.41901	309.46384
1.02800	322.15735	313.20844	310.45111	309.49384
1.03400	322.20755	313.24493	310.48230	309.52301
1.04000	322.25610	313.28040	310.51260	309.55139
1.04600	322.30313	313.31479	310.54208	309.57898
1.05200	322.34876	313.34818	310.57074	309.60584
1.05800	322.39304	313.38062	310.59857	309.63190
1.06400	322.43607	313.41205	310.62561	309.65729
1.07000	322.47788	313.44257	310.65192	309.68195
1.07600	322.51849	313.47214	310.67743	309.70590
1.08200	322.55792	313.50079	310.70221	309.72919
1.08800	322.59583	313.52850	310.72626	309.75177
1.09400	322.63507	313.55603	310.74994	309.77399